

# Critical point in heavy-quark QCD at finite temperature

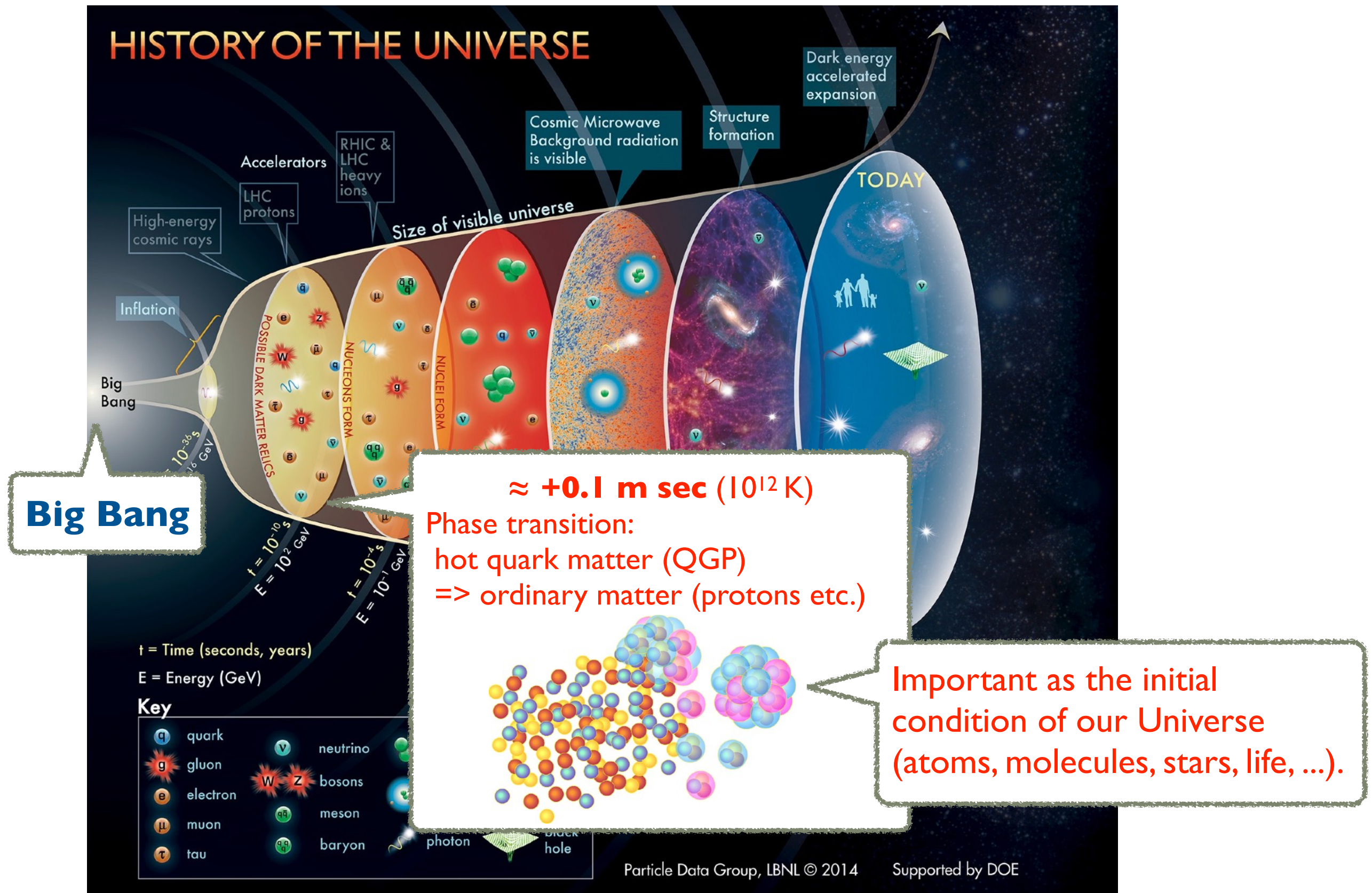
**Kazuyuki Kanaya<sup>1)</sup> with Ryo Ashikawa<sup>2)</sup>, Shinji Ejiri<sup>3)</sup>,  
Masakiyo Kitazawa<sup>2,4)</sup>, Hiroshi Suzuki<sup>5)</sup>, Naoki Wakabayashi<sup>3)</sup>  
(WHOT-QCD Collaboration)**

*1) Univ. Tsukuba, 2) Osaka Univ., 3) Niigata Univ., 4) Kyoto Univ., 5) Kyushu Univ.*



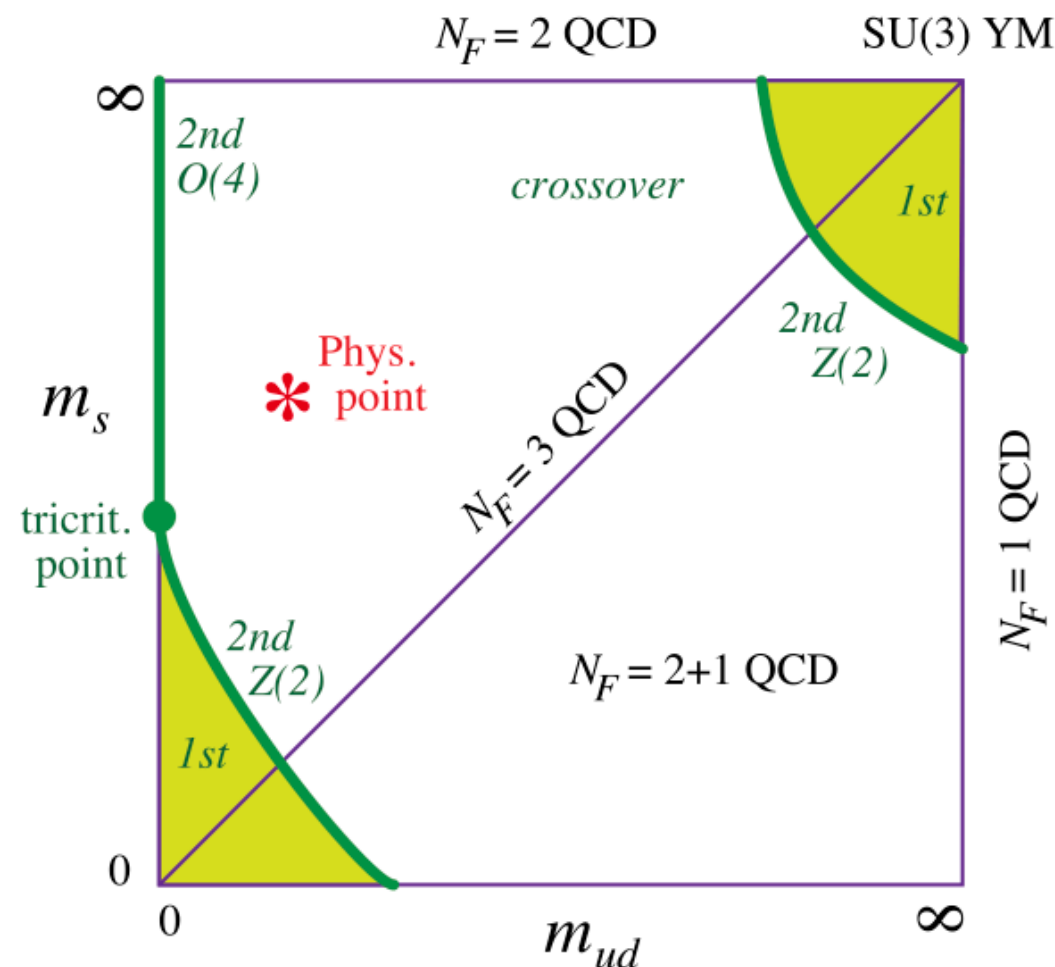


# QCD : the fundamental theory of quarks



# Nature of $T > 0$ QCD transition as function of $m_q$ 's

*The traditional picture given by this Columbia plot*



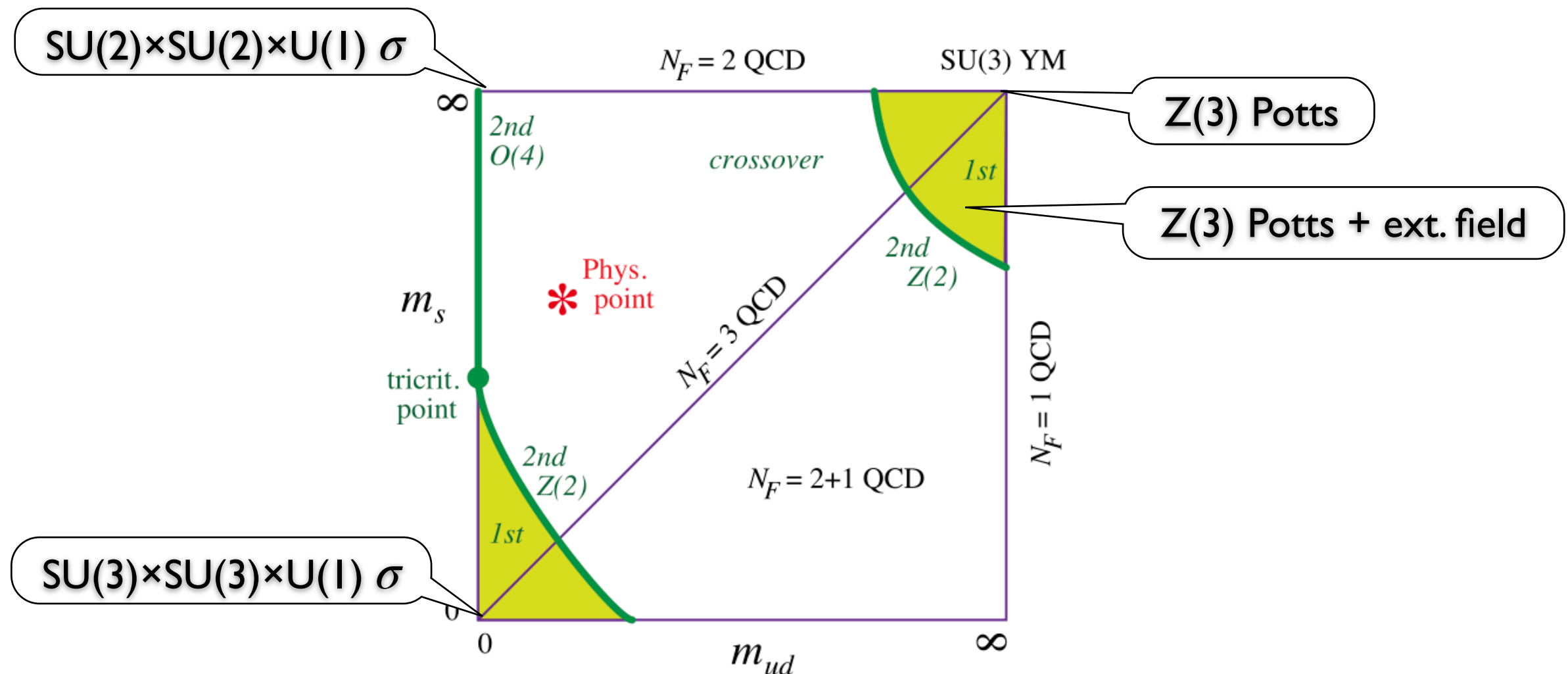
► The physical point locates in the crossover region.

Nature of the QCD transition off the phys. pt. is important

$\Leftarrow$  properties at the phys. pt. affected by scaling of nearby critical points.

# Nature of $T > 0$ QCD transition as function of $m_q$ 's

The traditional picture given by this Columbia plot



► Universality arguments with effective chiral  $\sigma$  model around the chiral limits

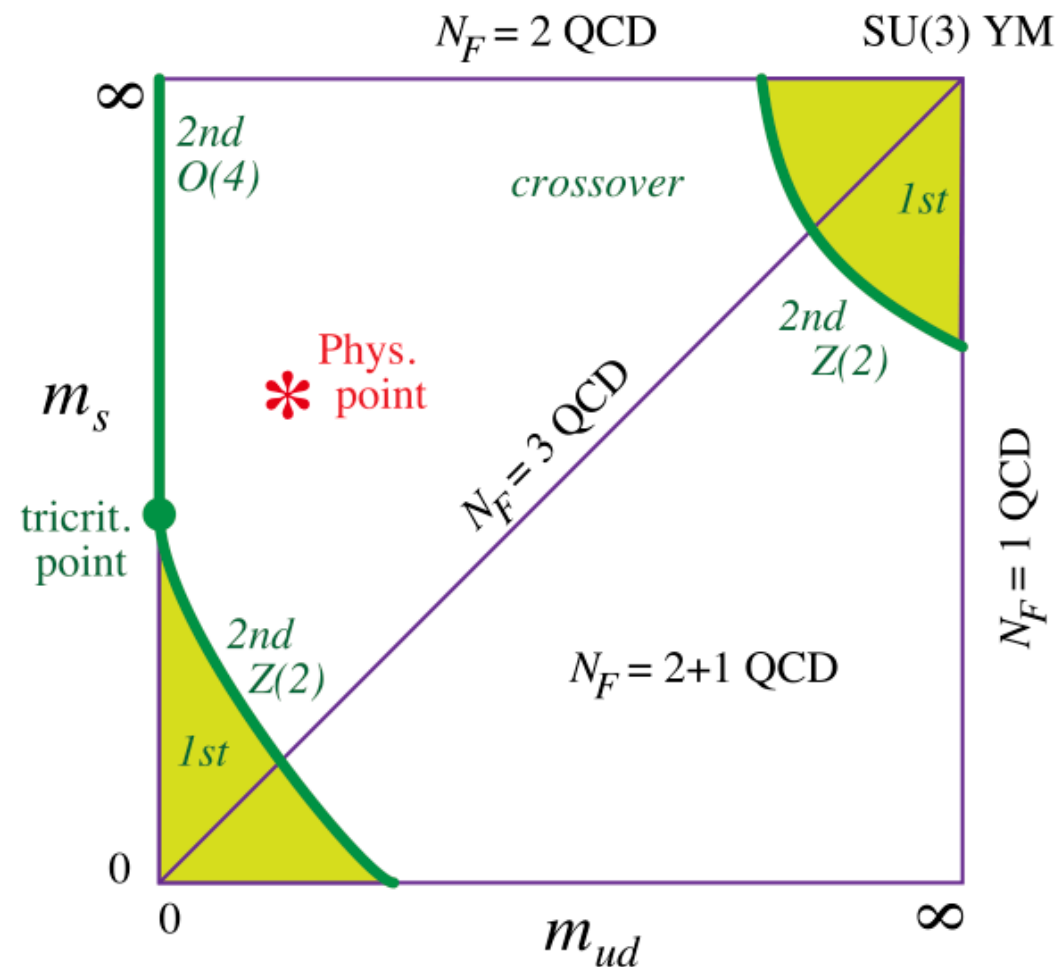
- Pisarski-Wilczek, Phys. Rev. D 29 (1984) 338
- Wilczek, Int. J. Mod. Phys. A7 (1992) 3911
- Rajagopal-Wilczek Nucl. Phys. B399 (1993) 395

$\Rightarrow N_f = 2$  : 2nd order in the  $O(4)$  univ. class //  $N_f \geq 3$  : 1st order



# Nature of $T > 0$ QCD transition as function of $m_q$ 's

The traditional picture given by this Columbia plot *is still under many discussions.*

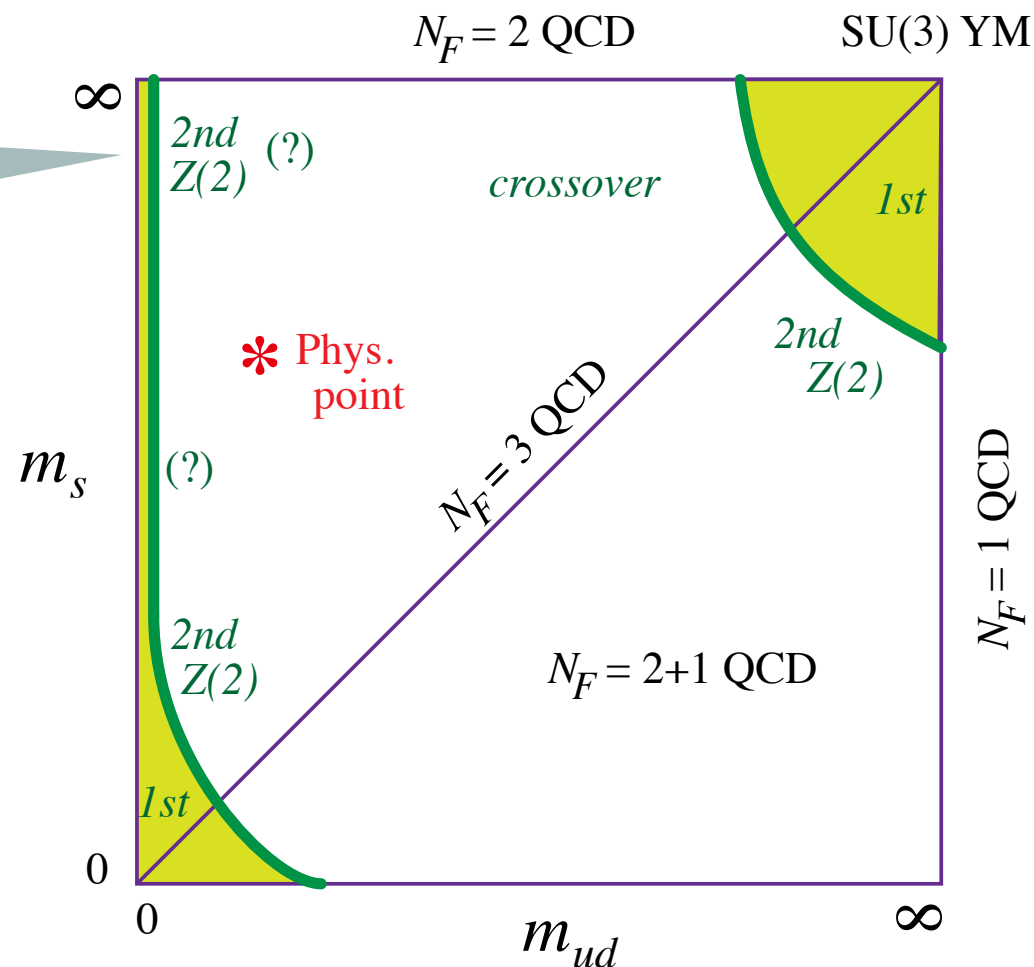


- If  $U(1)_A$  [broken by anomaly at all  $T$ 's] is *effectively* restored around  $T_c$ 
  - $\Rightarrow N_f = 2$  chiral trans. is either  $2^{nd}$  or  $1^{st}$
  - $\Rightarrow N_f = 3$   $1^{st}$  order region may be smaller [anomaly was a source of  $\phi^3$  pot.]

# Nature of $T > 0$ QCD transition as function of $m_q$ 's

The traditional picture given by this Columbia plot *is still under many discussions...*

Is the 2-flavor  
chiral limit 2nd  
order?



► 1st order for  $N_f = 2$   
on coarse lattices  
with unimproved  
lattice quarks

● D'Elia+, PRD 72 (2005);  
Cossu+, Lattice2008;  
Philipsen+Pinke, PRD 93  
(2016)

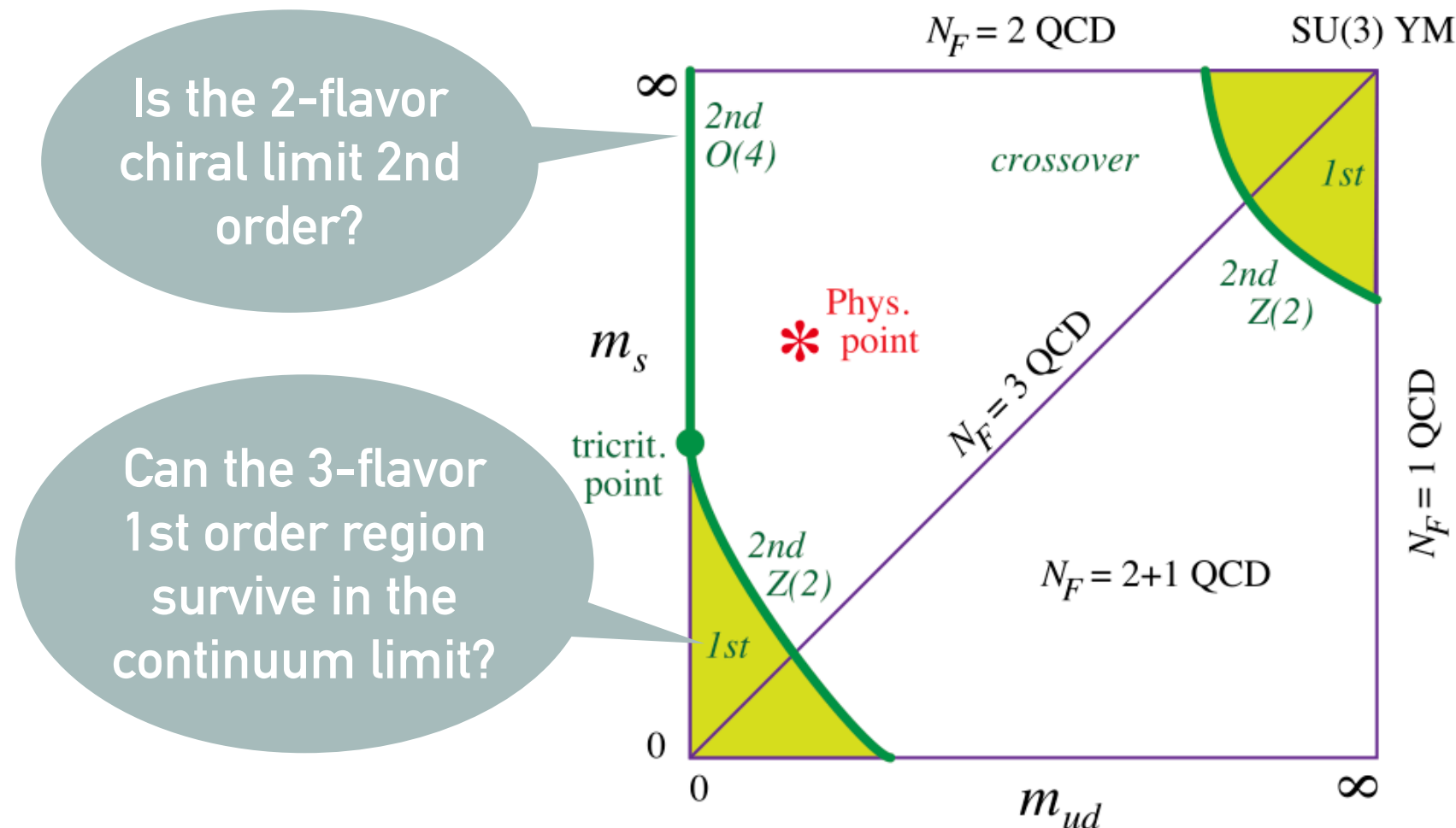
See also

● S.Aoki+, PRD 86 (2012)

- If  $U(1)_A$  [broken by anomaly at all  $T$ 's] is *effectively* restored around  $T_c$
- $\Rightarrow N_f = 2$  chiral trans. is either 2nd or 1st
  - $\Rightarrow N_f = 3$  1st order region may be smaller [anomaly was a source of  $\phi^3$  pot.]

# Nature of $T > 0$ QCD transition as function of $m_q$ 's

The traditional picture given by this Columbia plot *is still under many discussions...*

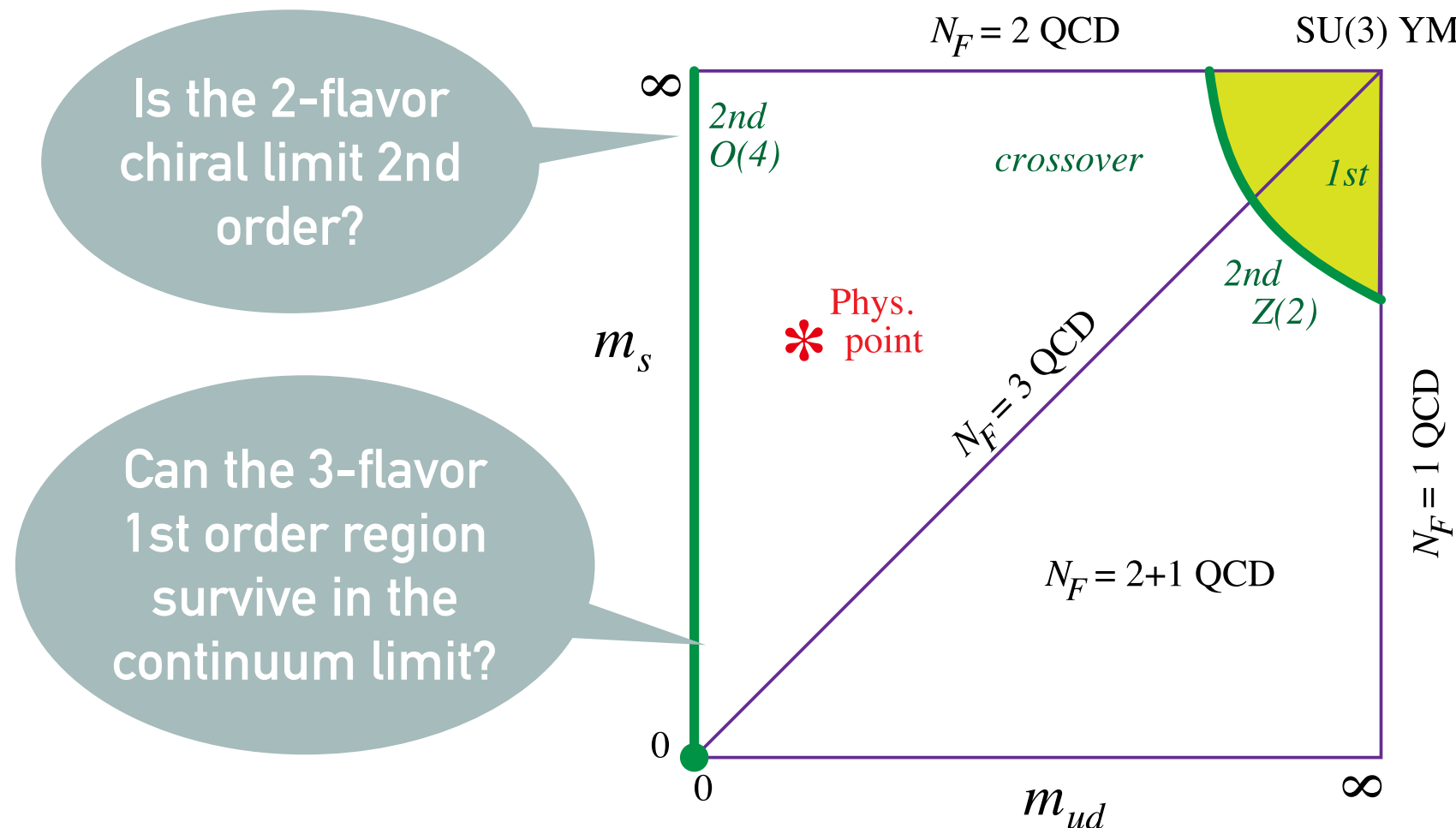


► Light-quark 1st order region for  $N_f \approx 3$  shrinks with  $a \rightarrow 0$  ( $N_t \rightarrow \infty$ )

- 🌐 Kuramashi+, *PRD* 101 (2020): improved Wilson,  $N_t=12$
- 🌐 Dini+, *PRD* 105 (2022): improved KS,  $N_t=8$

# Nature of $T > 0$ QCD transition as function of $m_q$ 's

The traditional picture given by this Columbia plot *is still under many discussions...*



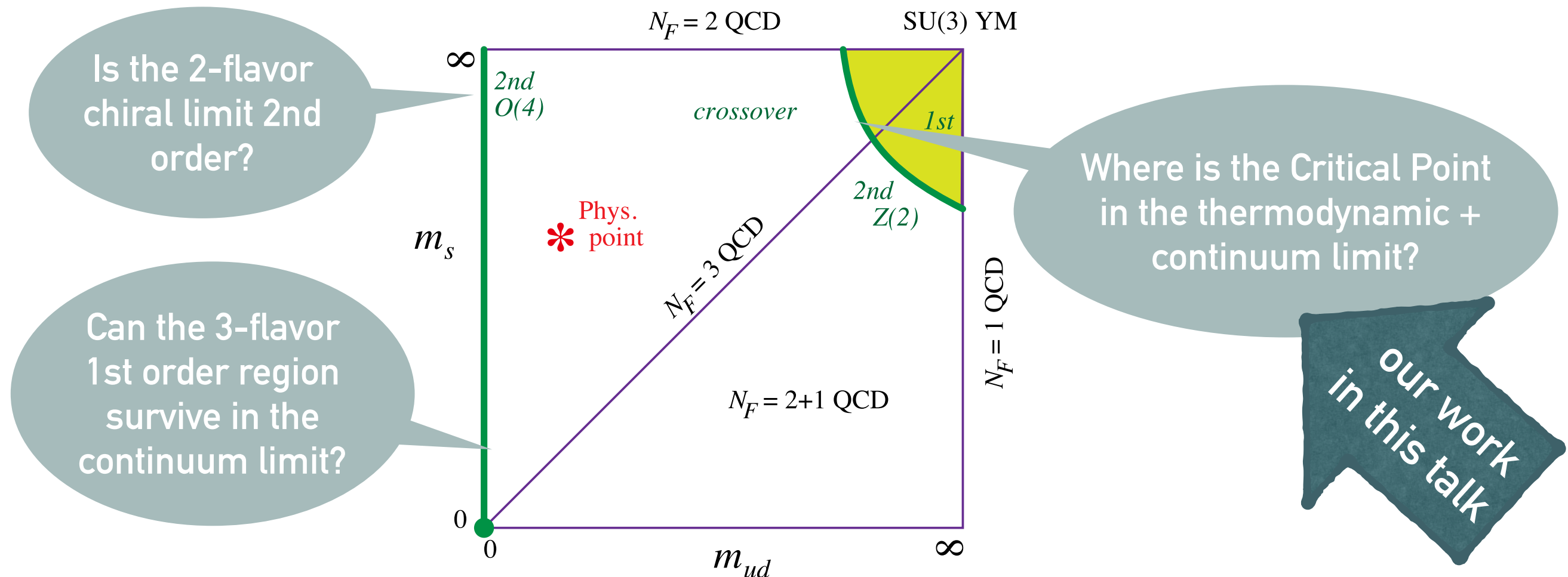
► Light-quark 1st order region for  $N_f \approx 3$  shrinks with  $a \rightarrow 0$  ( $N_t \rightarrow \infty$ )

- 🌐 Kuramashi+, *PRD* 101 (2020): improved Wilson,  $N_t=12$
- 🌐 Dini+, *PRD* 105 (2022): improved KS,  $N_t=8$



# Nature of $T > 0$ QCD transition as function of $m_q$ 's

The traditional picture given by this Columbia plot *is still under many discussions...*



## ► Recent studies on the location of CP in heavy-quark QCD

- Saito+ (WQHOT-QCD), *PRD* (2011/2014): HPE LO,  $N_t=4$ ,  $N_s/N_t=6$
- Ejiri+ (WHOT-QCD), *PRD* (2020): HPE eff-NLO,  $N_t=6$ ,  $N_s/N_t=4-6$ ;  $N_t=8$ ,  $N_s/N_t=3$
- Cuteri+, *PRD* (2021):  $N_f=2$ , fullQCD,  $N_t=6,8,10$ ,  $N_s/N_t=4-7(10)$

=> We still have strong cutoff & spatial volume dependences.

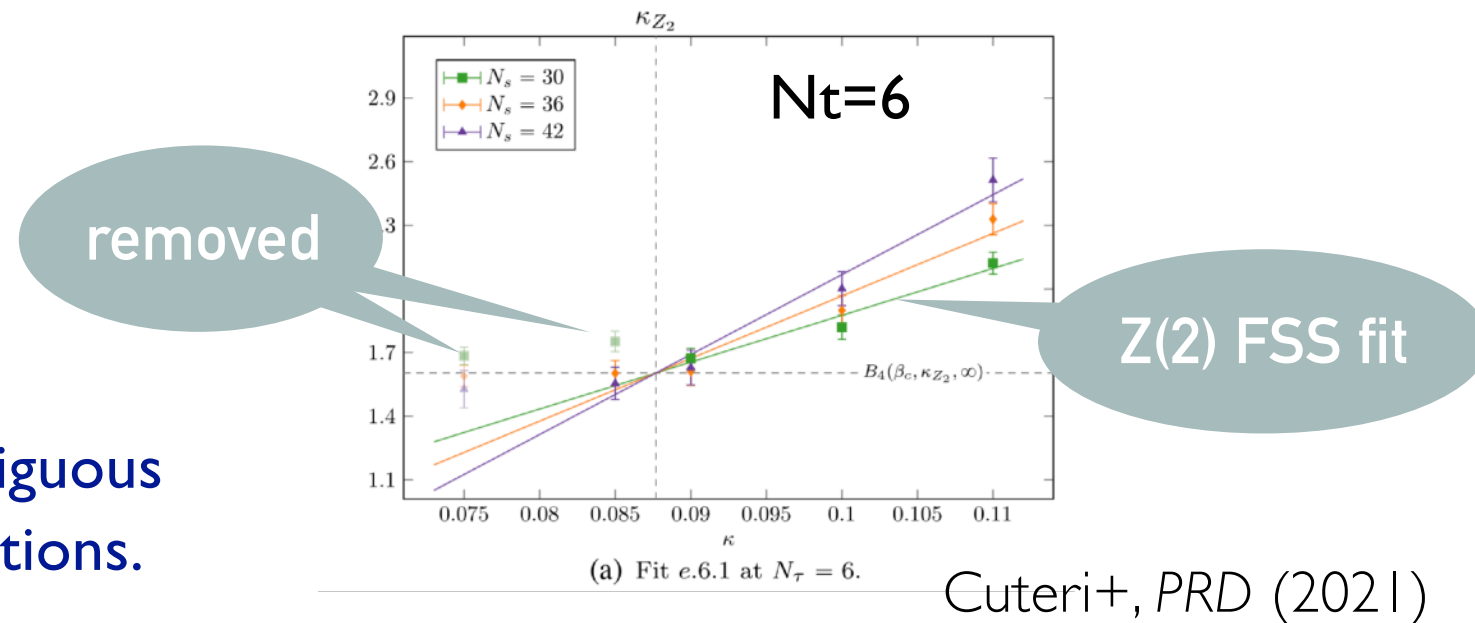
# Motivations

- Binder cumulant analysis based on the  $Z(2)$  FSS expected around CP

So far, however, identification of the  $Z(2)$  FSS is not a simple task

--- removal of many high-T data required / correction terms to the FSS introduced.

These make the analyses slightly ambiguous & call careful systematic error estimations.



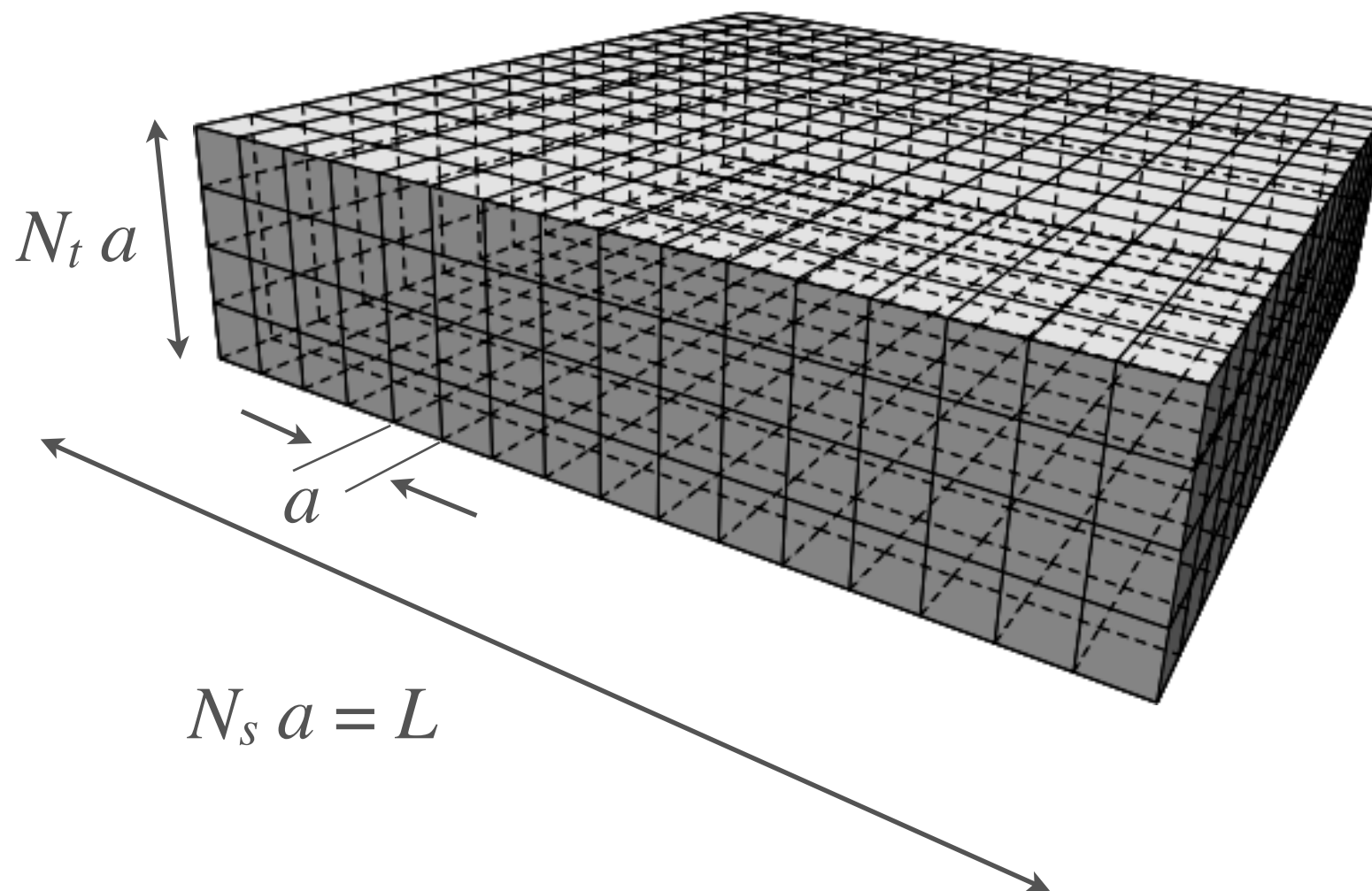
- => Simulations with larger spatial volumes & high statistics to identify the FSS more clearly.
- => Multi-point reweighting to vary coupling parameters continuously.

This talk is based on

- 🌐 Kiyohara+ (WQHOT-QCD), *Phys.Rev.D* (2021) [DOI: 10.1103/PhysRevD.104.114509]
- 🌐 Wakabayashi+ (WHOT-QCD), *Prog.Theor.Exp.Phys.* (2022) [DOI: 10.1093/ptep/ptac019]
- 🌐 Ashikawa+ (WHOT-QCD), *ongoing*

# Lattice setup

---



$$T = \frac{1}{N_t a}$$

$N_t$  : lattice size in the euclidian time direction

$a$  : lattice spacing

For a given  $T$ ,  
continuum limit:  $N_t \rightarrow \infty$

Spatial system size  $L = N_s a \leq$  we control it by the "aspect ratio"  $N_s / N_t = L T$ .

- previous studies :  $L T \approx 4 - 7$  (10)
- our study :  $L T$  up to 12 or 15

To suppress comp. costs on large spatial volumes, we first revisited  $N_t=4$  [Kiyohara+].  
We are now extending the study to  $N_t=6$  [Ashikawa+, ongoing].



# Lattice setup

► Our lattice action: plaquette gauge + standard Wilson quarks

► Wilson quark kernel: 
$$M_{xy}(\kappa) = \delta_{xy} - \kappa \sum_{\mu} \left[ (1 - \gamma_{\mu}) U_{x,\mu} \delta_{y,x+\hat{\mu}} + (1 + \gamma_{\mu}) U_{y,\mu}^{\dagger} \delta_{y,x-\hat{\mu}} \right]$$
  

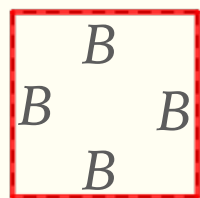
$$= \delta_{xy} - \kappa B_{xy}$$
 hopping term 
$$\kappa = \frac{1}{2am_q + 8}$$

► Quark contribution to the effective action:  $\ln \det M(\kappa) = -\frac{1}{N_{\text{site}} n} \sum_{n=1}^{\infty} \text{Tr}[B^n] \kappa^n$   
 • closed loops of  $B$  with  $\kappa$  [loop length]

► **Hopping Parameter Expansion** to **reduce simulation costs** for large spatial volumes

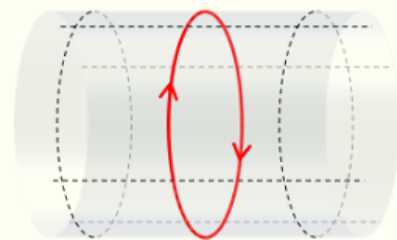
LO:

plaquette



$$\kappa^4$$

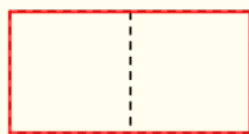
Polyakov loop  $\Omega$



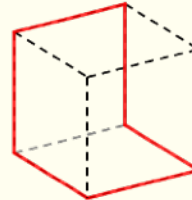
$$\kappa^{N_t}$$

NLO:

(a) rectangle

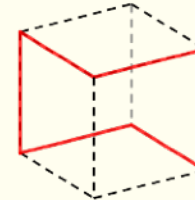


(b) chair

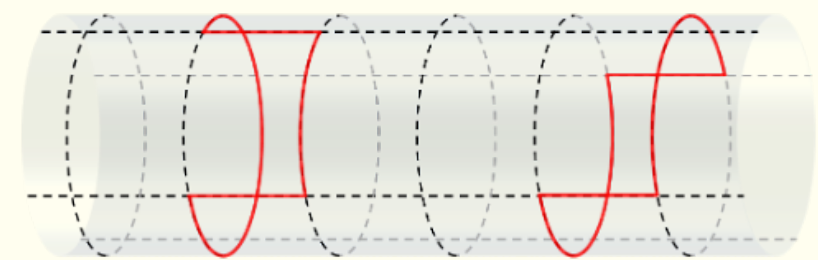


$$\kappa^6$$

(c) crown



bent Polyakov loops  $\Omega_i$



$$\kappa^{N_t+2}$$

• HPE  $\approx 1/(am_q)$  expansion

• HPE worsens with  $a \rightarrow 0$  ( $N_t \rightarrow \infty$ )  $\Rightarrow$  higher order terms required with  $N_t \rightarrow \infty$ .

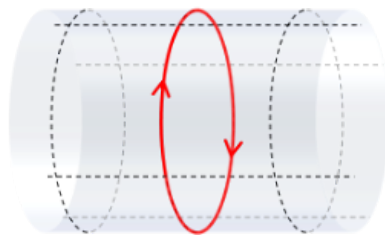
# Simulation incorporating LO + NLO meas.'s

Kiyohara, Kitazawa, Ejiri, KK (WHOT-QCD), PRD 104 (2021)

- LO incorporated in the configuration generation



$$\beta \rightarrow \beta^* = \beta + 48N_f\kappa^4$$



$$\lambda \sum_{\mathbf{x}} \Omega(\mathbf{x}) \text{ term in the effective action } (\lambda = 48N_fN_t\kappa^4 \text{ for } N_t=4)$$

can be incorporated in PHB+OR parallel simulation efficiently  
by keeping all temporal sites within a node

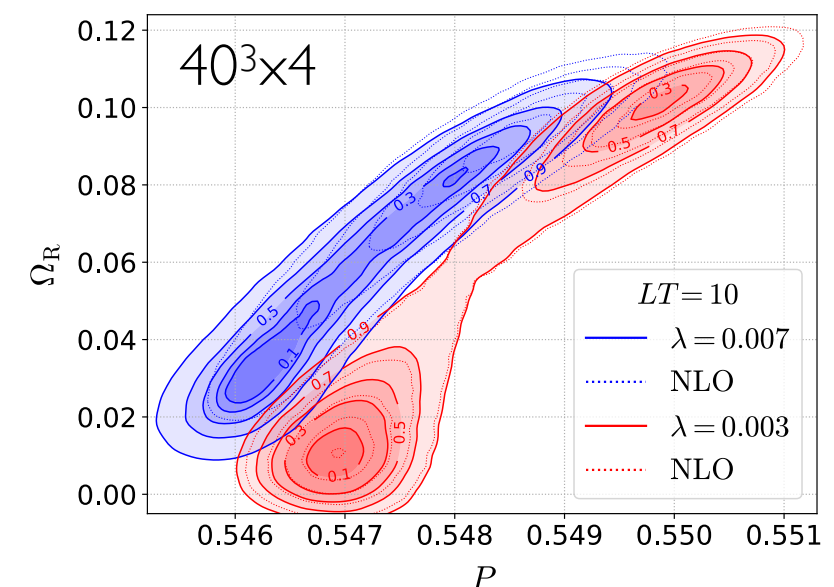
=> Simulation cost  $\leq 1/100$  of full-QCD simulations : large spatial volume enabled

- NLO incorporated in the measurements through multi-point reweighting

$$\langle \hat{O}(U) \rangle_{\beta, \lambda}^{\text{NLO}} = \frac{\langle \hat{O}(U) e^{-\delta S_{\text{LO}} - S_{\text{NLO}}(\beta, \lambda)} \rangle_{\tilde{\beta}, \tilde{\lambda}}^{\text{LO}}}{\langle e^{-\delta S_{g+\text{LO}} - S_{\text{NLO}}(\beta, \lambda)} \rangle_{\tilde{\beta}, \tilde{\lambda}}^{\text{LO}}}$$

$$\delta S_{g+\text{LO}} = S_{g+\text{LO}}(\beta, \lambda) - S_{g+\text{LO}}(\tilde{\beta}, \tilde{\lambda})$$

- Simulations at several  $(\tilde{\beta}^*, \tilde{\lambda}) \Rightarrow$  measure at  $(\beta^*, \lambda)$
- Overlap problem resolved by the inclusion of LO in configuration generations <= essential on spatially large lattices in this study

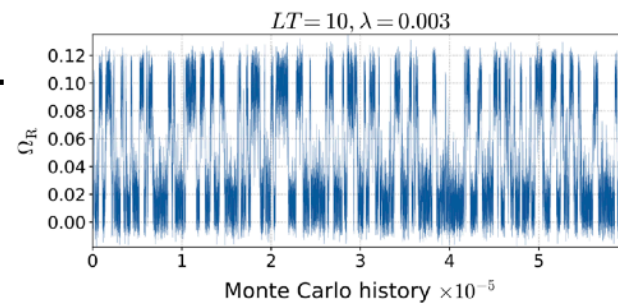


# Study on $N_t = 4$ lattices

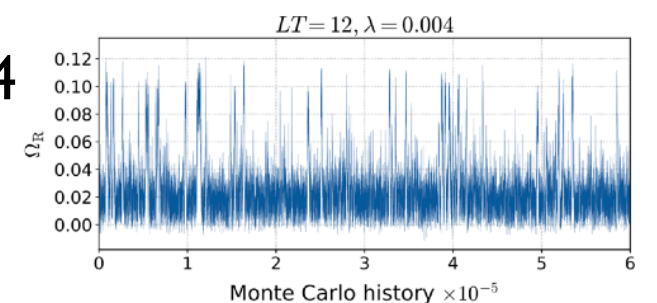
Kiyohara, Kitazawa, Ejiri, KK (WHOT-QCD), *PRD* 104 (2021)

- ▶ Simulations:  $N_t=4$ ,  $N_s/N_t = LT = 6, 8, 9, 10, 12$ , each  $3-6 \times [(\tilde{\beta}^*, \tilde{\lambda})$  with  $\sim 10^6$  meas.] around the transition line  
 $L$  = spatial lattice size,  $\lambda = 48N_f N_t \kappa^4$  for  $N_t=4$

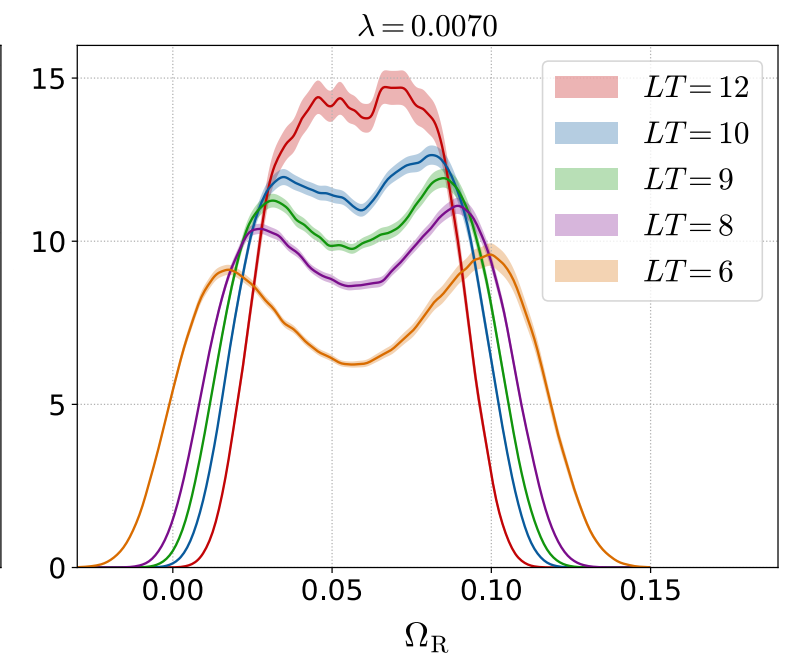
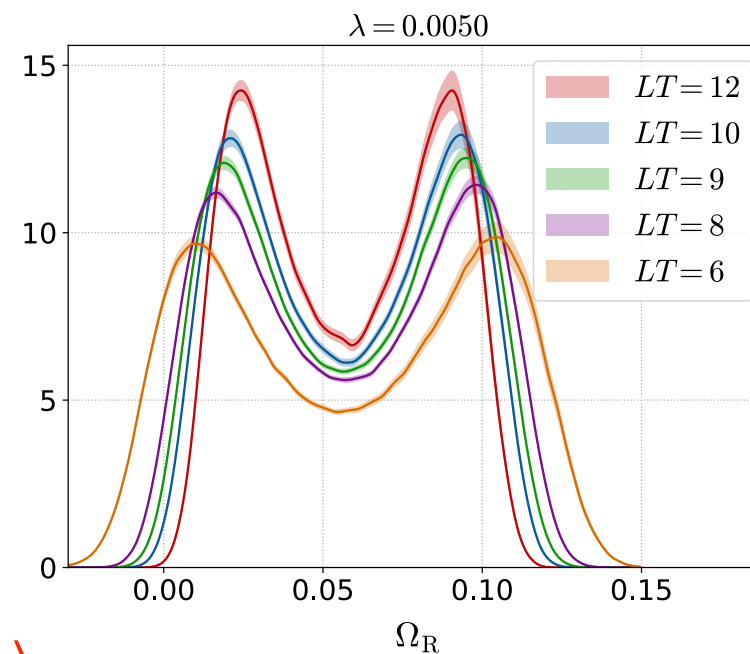
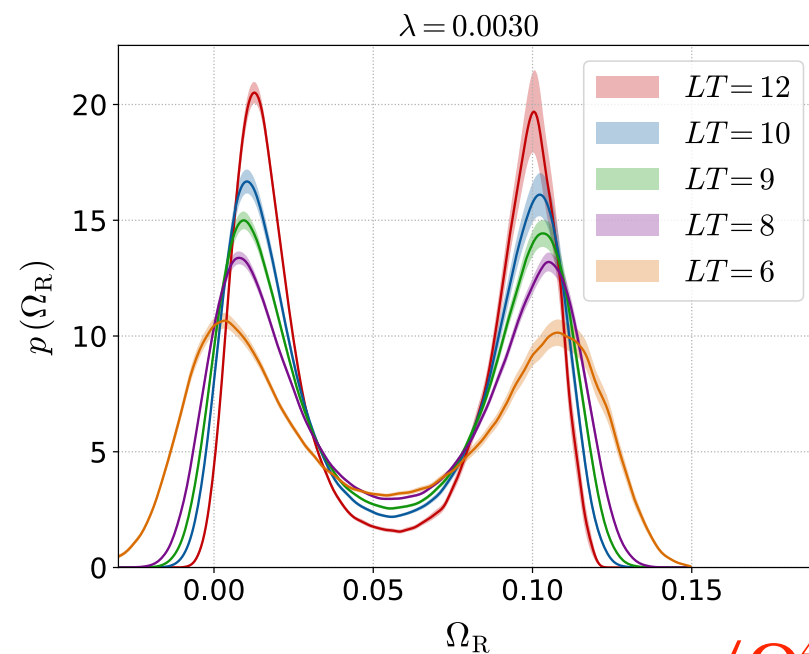
- ▶ History of  $\Omega_R = \text{Re}\Omega$   $40^3 \times 4$



$48^3 \times 4$



- ▶ Distribution of  $\Omega_R$  on the transition line



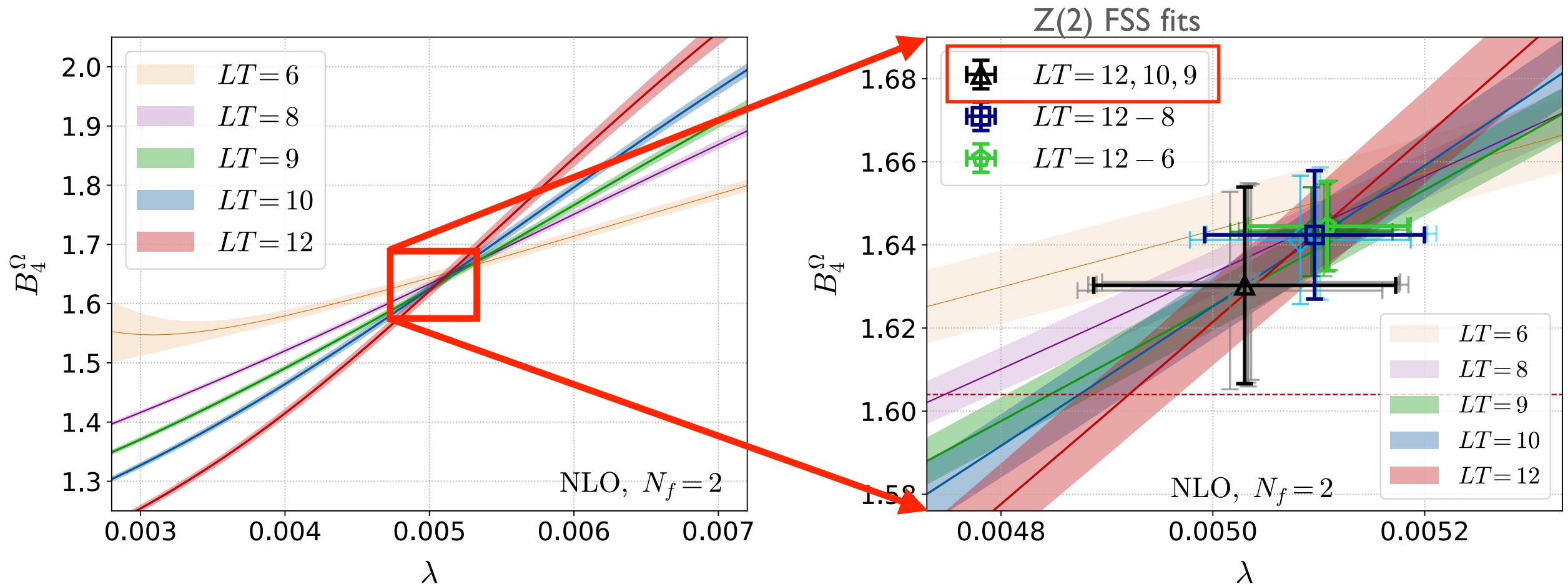
=> Binder cumulant  $B_4^\Omega = \frac{\langle \Omega_R^4 \rangle_c}{\langle \Omega_R^2 \rangle_c^2} + 3$  along the transition line in the  $(\beta, \kappa)$  plane.



# Study on $N_t = 4$ lattices

Kiyohara, Kitazawa, Ejiri, KK (WHOT-QCD), *PRD* 104 (2021)

## ► Results at $N_t=4$ with HPE up to NLO



- ★ Precision much improved over previous studies
- ★  $N_s/N_t = LT \geq 9$  required for Z(2) FSS
- ★  $B_4^\Omega = 1.630(24)(2)$  using  $N_s/N_t \geq 9$ , consistent with Z(2) value 1.604 within  $\approx 1\sigma$
- ★  $\lambda_c = 0.00503(14)(2)$  [ $\kappa_c = 0.0603(4)$ ] for  $N_t=4, N_f=2$

(cf.) Ejiri+ *PRD*(2020):  $\kappa_c = 0.0640(10)$  with eff. NLO

# Scope and convergence of HPE

Wakabayashi, Ejiri, KK, Kitazawa (WHOT-QCD), PTEP (2022)

*Are the effects of further higher orders of HPE really negligible?*

► Quark contribution to the effective action:

loops of length n

noise average

$$\ln \det M(\kappa) = N_{\text{site}} \sum_n D_n \kappa^n, \quad D_n = \frac{-1}{N_{\text{site}} n} \text{Tr}[B^n] \approx \frac{-1}{N_{\text{site}} n} \langle \langle \eta^\dagger B^n \eta \rangle \rangle_{\text{noises}}$$

$$B_{xy} = \sum_\mu \left[ (1 - \gamma_\mu) U_{x,\mu} \delta_{y,x+\hat{\mu}} + (1 + \gamma_\mu) U_{y,\mu}^\dagger \delta_{y,x-\hat{\mu}} \right]$$

Wilson-type loops

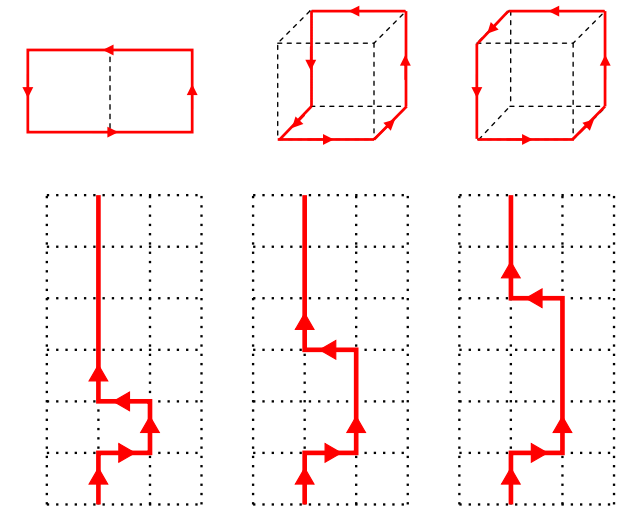
$$W(4) = 96 N_c \hat{P}, \quad W(6) = 256 N_c (3 \hat{W}_{\text{rec}} + 6 \hat{W}_{\text{chair}} + 2 \hat{W}_{\text{crown}})$$

$$D_n = W(n) + \sum_m L_m(N_t, n) = W(n) + L(N_t, n)$$

Polyakov-type loops with m-windings

$$L_1(N_t, N_t) = \frac{4 N_c 2^{N_t}}{N_t} \text{Re} \hat{\Omega}$$

$$L_1(N_t, N_t + 2) = 12 N_c 2^{N_t} \sum_k \text{Re} \hat{\Omega}_k$$



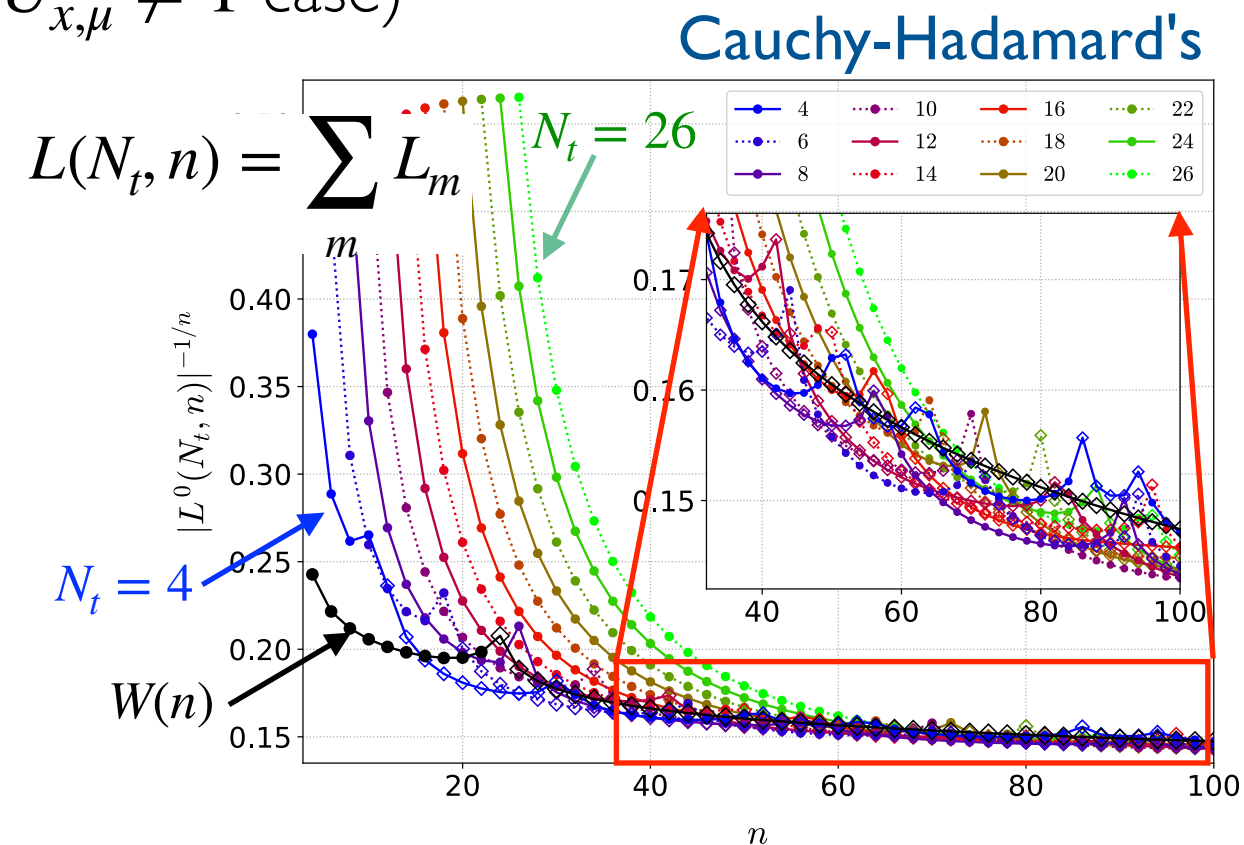
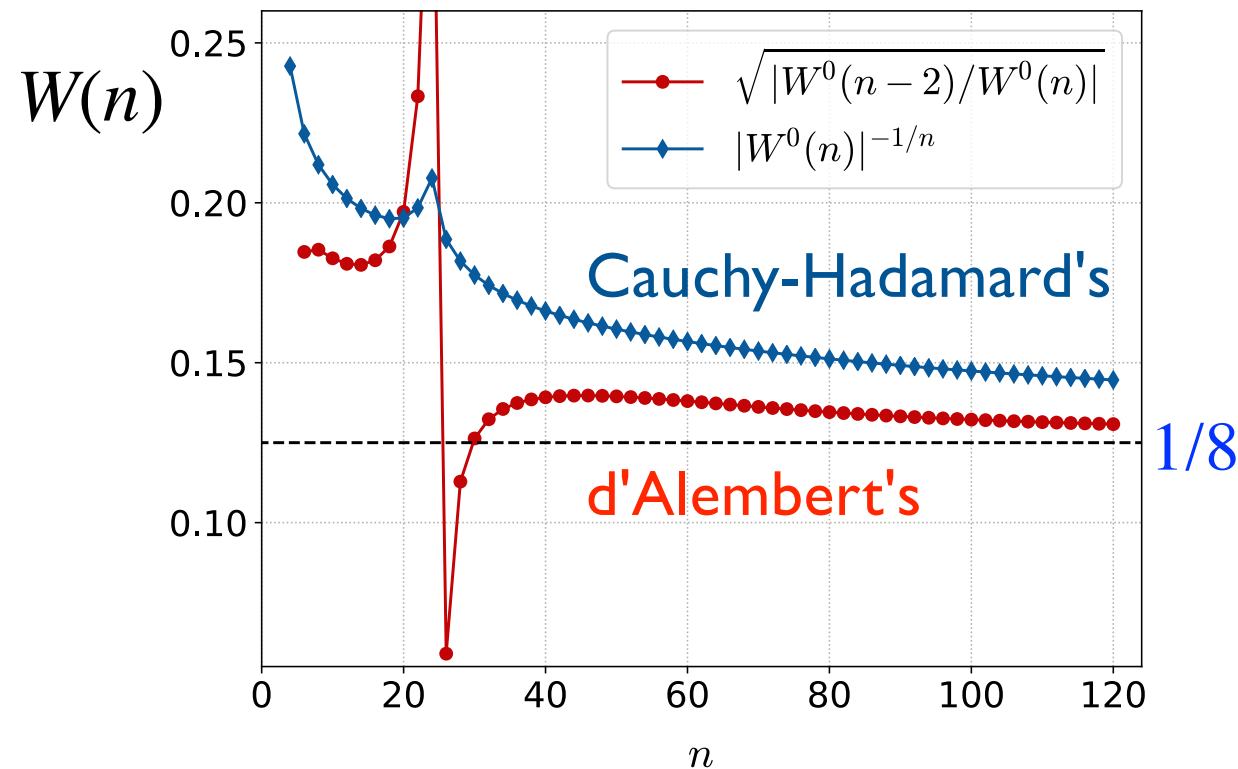
We developed a method to separately evaluate  $W(n)$  and  $L_m(N_t, n)$  from  $D_n$  by combining the results with various twisted boundary conditions.

# Scope and convergence of HPE

Wakabayashi, Ejiri, KK, Kitazawa (WHOT-QCD), *PTEP* (2022)

- $\hat{W}_i, \hat{P}_j$  in  $W(n)$  and  $L_m(N_t, n)$  take their maximum value 1 when we set  $U_{x,\mu} = 1$   
 In this case, we can calculate  $W(n)$  and  $L_m(N_t, n)$  analytically up to high orders.  
 => **Worst convergent case of HPE can be studied by combining them.**

◆ Convergence radius (lower bound for the  $U_{x,\mu} \neq 1$  case)



★ Convergence radius  $\xrightarrow{n \rightarrow \infty} 1/8$ , i.e. convergent up to the chiral limit.

<= free Wilson quarks when  $U_{x,\mu} = 1$

=> HPE reliable at any  $m_q$ , when sufficiently high orders are taken.

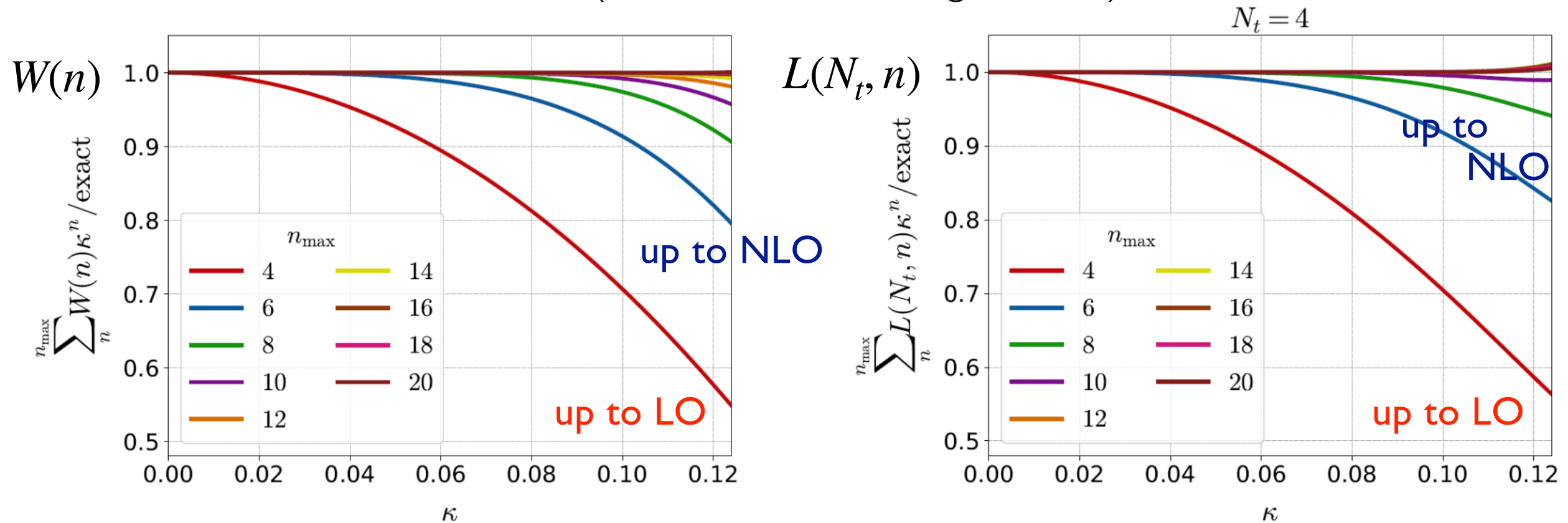


# Scope and convergence of HPE

Wakabayashi, Ejiri, KK, Kitazawa (WHOT-QCD), *PTEP* (2022)

To which order we need to incorporate?  $\leq$  depends on the value of  $\kappa$

◆ Deviation due to truncation (in the worst convergent case):



★ For  $N_t=4$ :  $\kappa_c = 0.0603(4)$  [Kiyohara+ ('21)]

=> LO may have at worst  $\approx 10\%$  error, NLO good enough

★ For  $N_t=6$ :  $\kappa_c = 0.0877(9)$  [Cuteri+ ('22)],  $0.1286(40)$  [Ejiri+ ('20) using eff. pot.]

=> NLO is  $\geq 93\%$  accurate. remaining error can be removed by NNLO or higher

★ For  $N_t=8$ :  $\kappa_c = 0.1135(8)$  [Cuteri+ ('22)]

=> NNLO needed for  $\geq 95\%$  accuracy

# Effective method to incorporate high orders

Wakabayashi, Ejiri, KK, Kitazawa (WHOT-QCD), *PTEP* (2022)

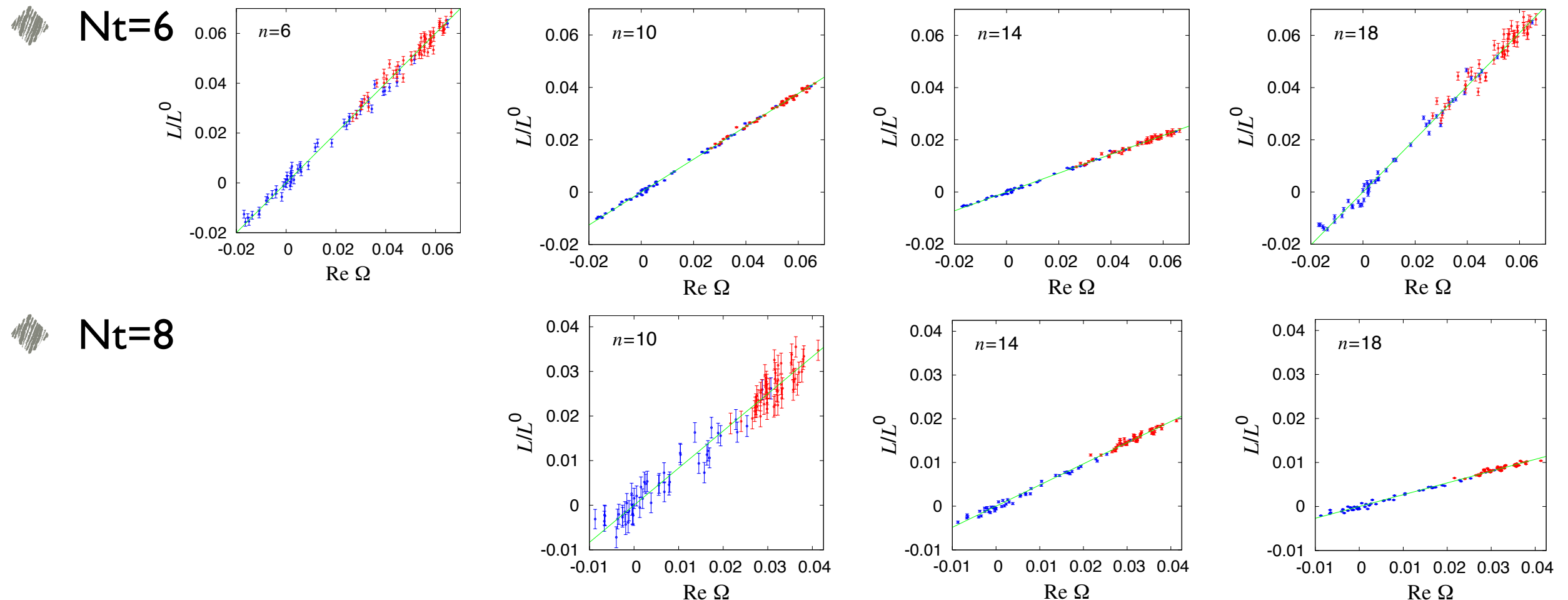
*Calcuration of high order term becomes quickly difficult with increasing  $n$ .*

We extend the idea of the effective NLO method [Ejiri+ ('20)] to high orders.

Basic observation: **strong correlation of Wilson/Polyakov-type loops among different  $n$ .**

## ► Distribution of $L(N_t, n)$ vs. the Polyakov loop $\Omega$

- qQCD simulation on  $32^3 \times (6, 8)$ , blue/red slightly below/above  $\beta_{\text{trans}}$
- normalized by the  $U \times \mu = 1$  result  $L^0$



# Effective method to incorporate high orders

Wakabayashi, Ejiri, KK, Kitazawa (WHOT-QCD), *PTEP* (2022)

This linear correlation suggests us to approximate

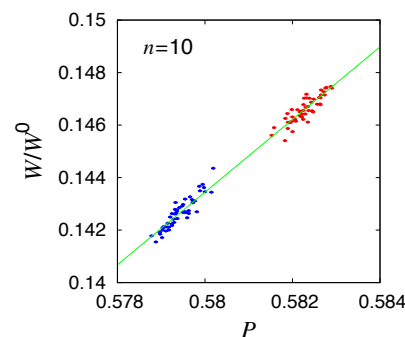
★  $L(N_t, n) \approx L^0(N_t, n) c_n \text{Re}\hat{\Omega}$

known from  $U_{x\mu}=1$

slope  
measured by  
simulation

	$N_t = 6$	$N_t = 8$
$c_6$	1	
$c_8$	0.8112(20)(7)	1
$c_{10}$	0.6280(15)(3)	0.8327(114)(95)
$c_{12}$	0.4736(29)(15)	0.6408(36)(27)
$c_{14}$	0.3609(26)(11)	0.4841(22)(10)
$c_{16}$	0.3106(25)(10)	0.3616(21)(6)
$c_{18}$	1.0159(90)(33)	0.2679(16)(3)
$c_{20}$	-0.02771(57)(13)	0.2020(13)(2)

★  $W(n) \approx W^0(n) (d_n \hat{P} + f_n)$



though the correlation  
weaker than  $L(N_t, n)$

$n$	$d_n(N_t = 6)$	$f_n(N_t = 6)$	$d_n(N_t = 8)$	$f_n(N_t = 8)$
4	1	0	1	0
6	1.3625(73)(12)	-0.4070(42)(7)	1.3366(66)(8)	-0.3922(39)(5)
8	1.4644(123)(11)	-0.6089(72)(6)	1.4256(96)(8)	-0.5869(57)(5)
10	1.3835(156)(10)	-0.6590(91)(6)	1.3433(117)(8)	-0.6367(70)(5)
12	1.2140(178)(9)	-0.6235(103)(5)	1.1752(130)(7)	-0.6025(78)(4)
14	1.0256(196)(9)	-0.5533(114)(5)	0.9825(141)(7)	-0.5303(85)(4)
16	0.8607(219)(9)	-0.4811(127)(5)	0.8052(153)(8)	-0.4512(92)(5)
18	0.7481(258)(10)	-0.4296(150)(6)	0.6698(173)(9)	-0.3870(103)(5)
20	0.7290(337)(12)	-0.4275(196)(7)	0.6071(219)(12)	-0.3606(131)(7)

=> Higher order effects can be effectively incorporated in the LO simulation by

$$\beta \rightarrow \beta^* = \beta + \frac{1}{6} N_f \sum_{n=4}^{n_{\max}} W^0(n) d_n \kappa^n \quad \lambda \rightarrow \lambda^* = N_f N_t \sum_{n=N_t}^{n_{\max}} L^0(N_t, n) c_n \kappa^n$$

Extension to non-degenerate cases ( $N_f=2+1$  etc.) straightforward.



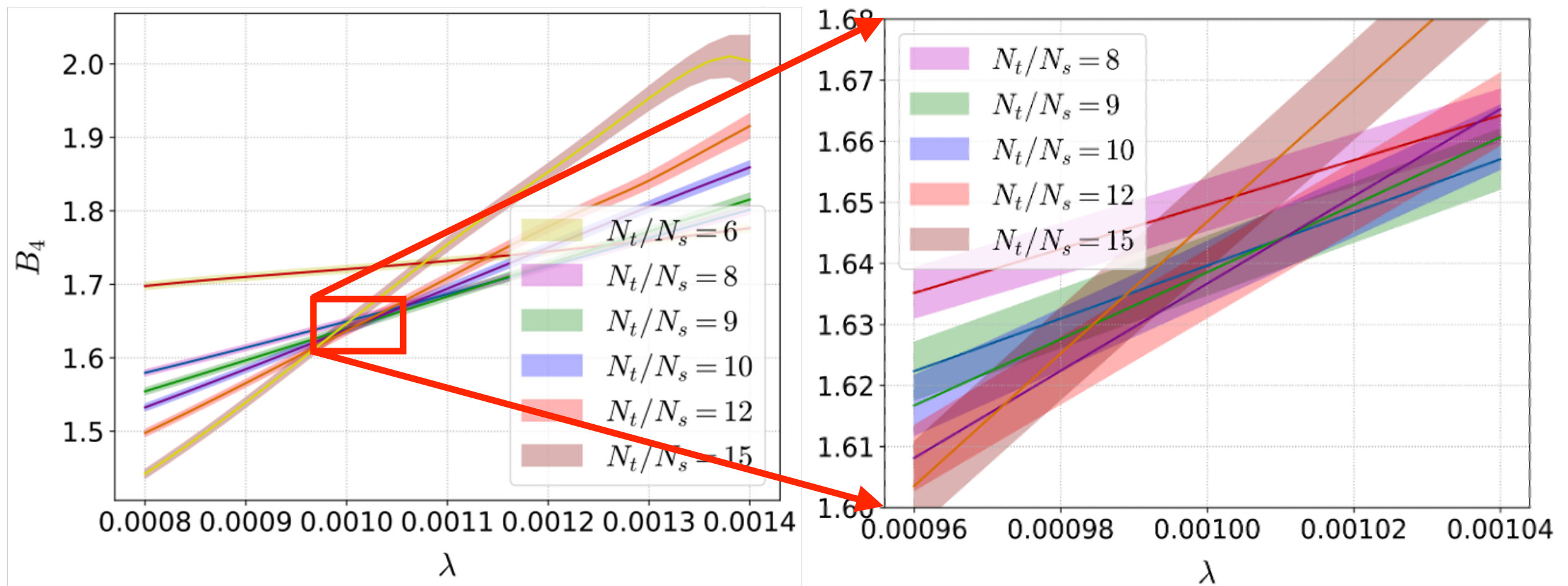
# Study on $N_t = 6$ lattices

Ashikawa+ (WHOT-QCD), *ongoing*

►  $N_t=6$ ,  $N_s/N_t = LT = 6, (7,) 8, 9, 10, 12, 15$  *ongoing*

► Status of  $B_4^\Omega$  with NLO:

$$\lambda = 128N_fN_t\kappa^6 \text{ for } N_t=6, N_f=2, \text{NLO}$$



*Preliminary:*

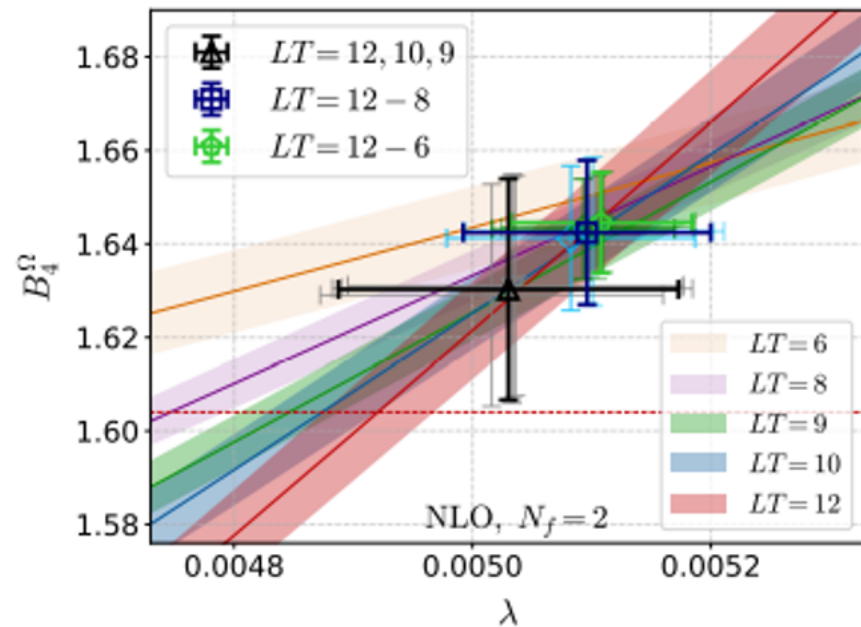
★  $B_4^\Omega \sim 1.61 - 1.62$  with  $N_s/N_t = 12-15$  (cf.)  $Z(2)$  value = 1.604

★  $\lambda_c \sim 0.00097 - 0.00101 \Rightarrow \kappa_c \sim 0.093$  NLO  $\Rightarrow \kappa_c \sim 0.0905$  up to 20th order  
(cf.)  $\kappa_c = 0.0877(9)$  by a full QCD simulation [Cuteri+ ('22)]

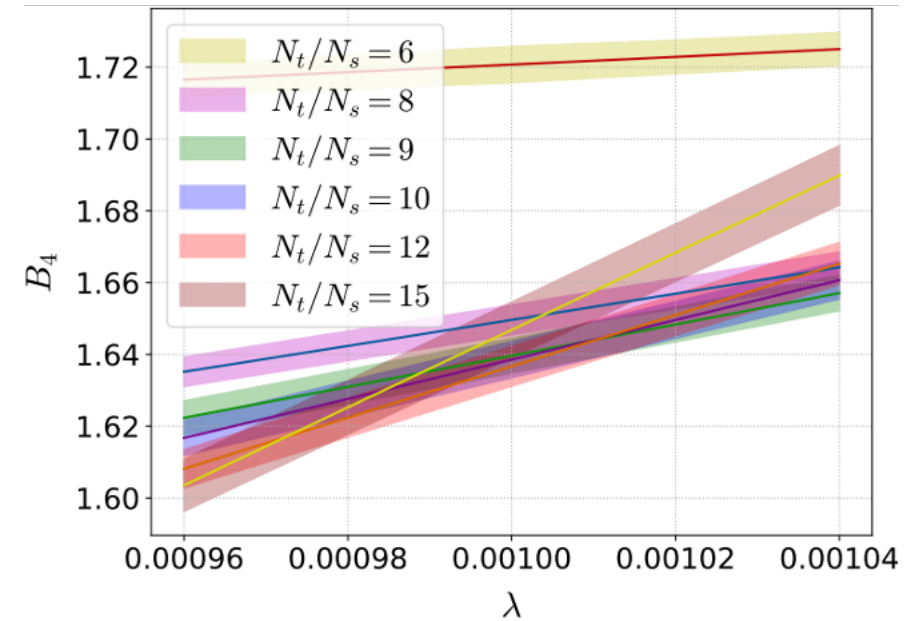
# $N_t = 4$ vs. $N_t = 6$

Ashikawa+ (WHOT-QCD), *ongoing*

$N_t = 4$



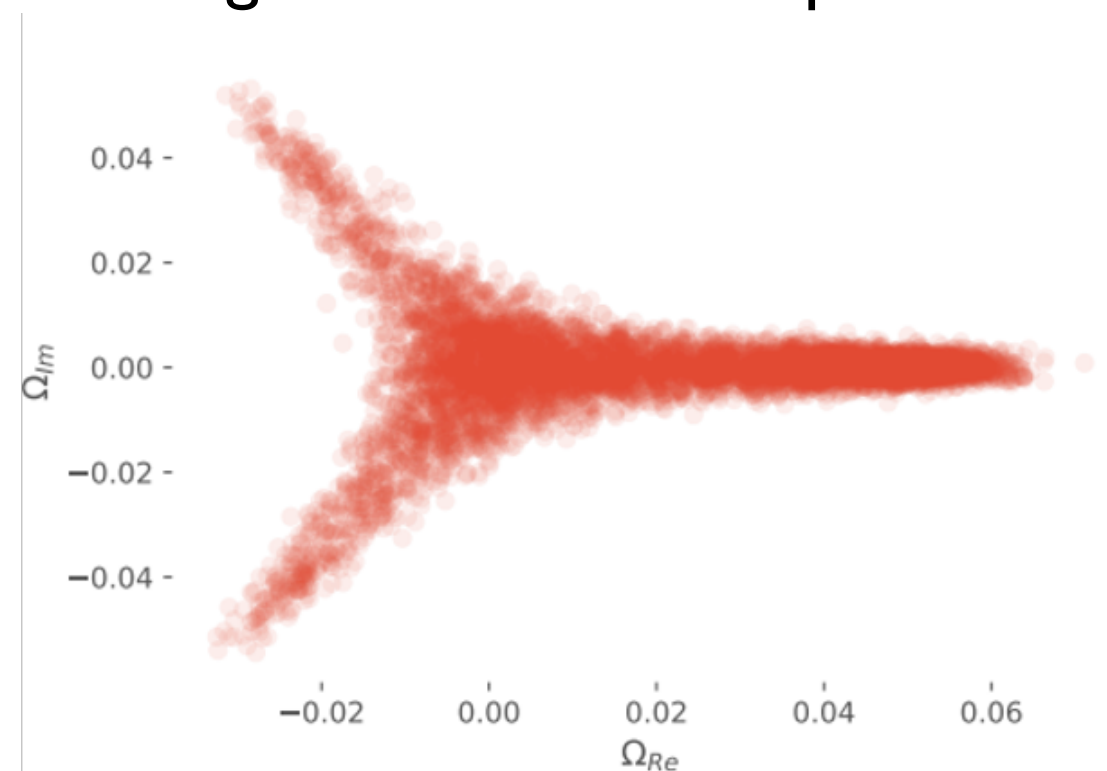
$N_t = 6$



★ Violation of FSS larger on finer lattice  $\Rightarrow$  larger  $N_s/N_t = LT$  required

## Origin of the violation:

- Contamination of remnant  $Z(3)$  distribution from  $m_q = \infty$  ?
- Mixing with energy-like op. in the scaling ??



# Conclusion & outlook

---

## ★ **HPE provides us with a reliable and powerful way to study QCD with heavy quarks**

- ☑ Convergent up to chiral limit + enable large  $N_s/N_t$  simul.'s + analytic in  $N_f$
- ☑ up to  $\kappa_c$  of  $N_t=4, N_f=2$  : LO:  $\geq 90\%$  / NLO:  $\geq 99\%$  accurate
- ☑ around  $\kappa_c$  of  $N_t=6, N_f=2$  : NLO:  $\geq 93\%$  accurate

Higher orders needed to remove remaining truncation error and for  $N_t \geq 8$ .

## ★ **Effective method to incorporate high orders developed** => reduce simulation cost largely

## ★ **At $N_t=4$ , $N_s/N_t \geq 9$ needed for $Z(2)$ FSS.**

=> NLO study of  $B_4^\Omega$  :  $\kappa_c = 0.0603(4)$  for  $N_f=2$

## ★ **At $N_t=6$ , larger violation of FSS, require larger $N_s/N_t$**

Preliminary with  $N_s/N_t \geq 12$ ,  $\kappa_c \sim 0.090$  including high orders.

🌀  $N_t=6$  ongoing: more statistics.

🌀 HPE powerful also at **finite densities**: in progress



.....

We miss our best friend+collaborator  
Yusuke Taniguchi  
who passed away on July 22, 2022.



1968–2022



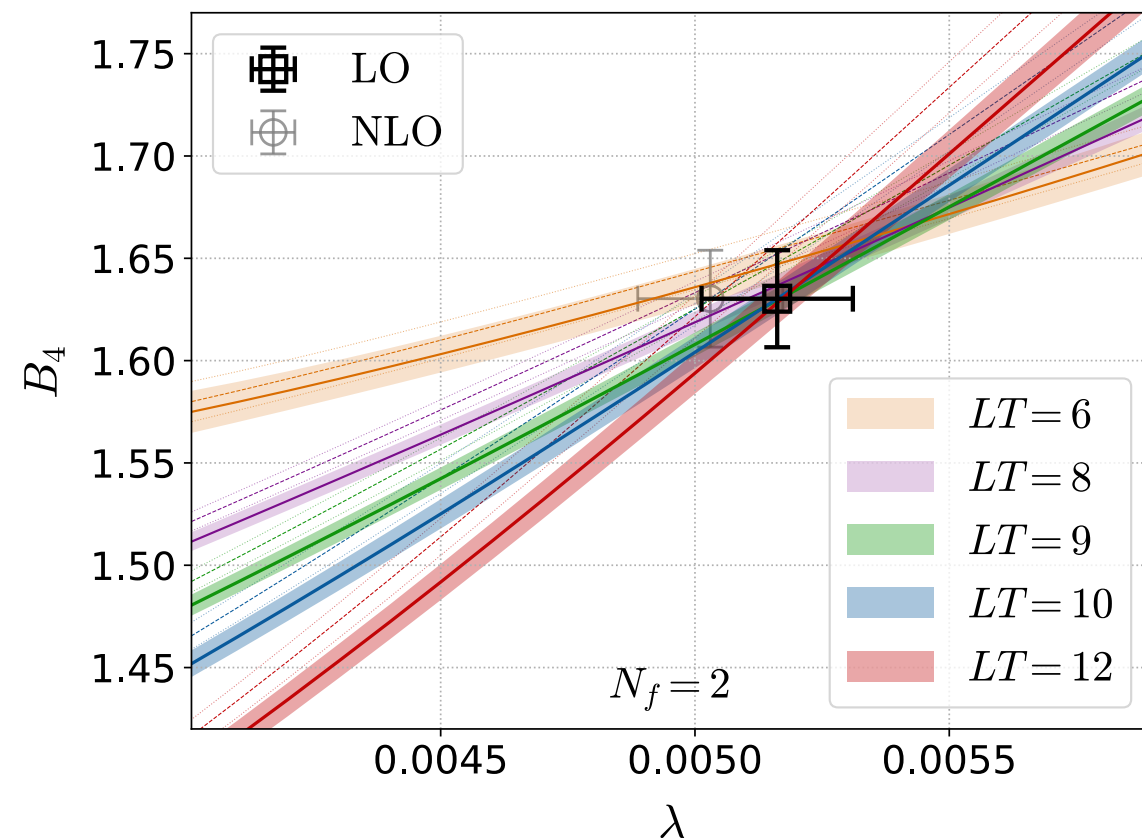
# backup slides



# Study on $N_t = 4$ lattices

Kiyohara, Kitazawa, Ejiri, KK (WHOT-QCD), *PRD* 104 (2021)

► Comparison with LO analysis  $\Rightarrow$  effects of NLO corrections



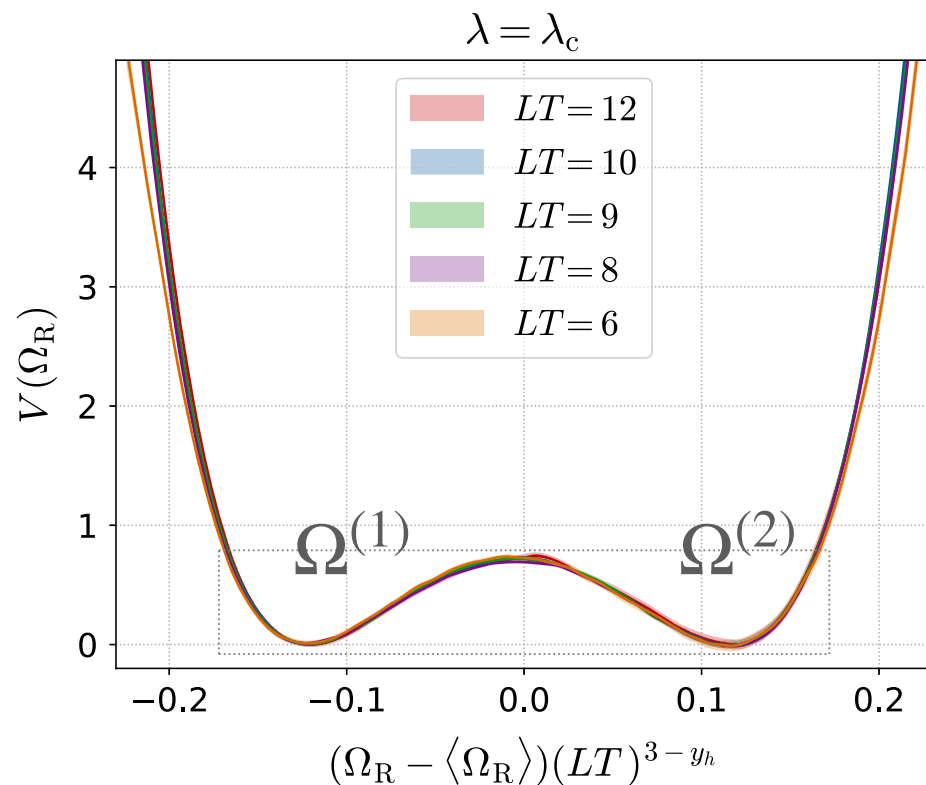
★ LO  $\approx$  NLO with  $N_s/N_t = LT \geq 9$

★ Shift due to NLO is small ( $\approx 2.6\%$ ), suggesting LO dominance around  $\kappa_c$  for  $N_t=4$   
 $\Rightarrow$  previous  $N_t=4$  LO results seems OK

# backup slides

Kiyohara, Kitazawa, Ejiri, KK (WHOT-QCD), *PRD* 104 (2021)

$$V(\Omega_R; \lambda, LT) = -\ln p(\Omega_R)_{\lambda, LT},$$



$$\Delta\Omega = \Omega^{(2)} - \Omega^{(1)}. \quad (46)$$

According to Eq. (15), this quantity should behave around the *CP* as

$$\Delta\Omega(\lambda, LT) = (LT)^{y_h-3} \Delta\tilde{\Omega}((\lambda - \lambda_c)(LT)^{1/\nu}), \quad (47)$$

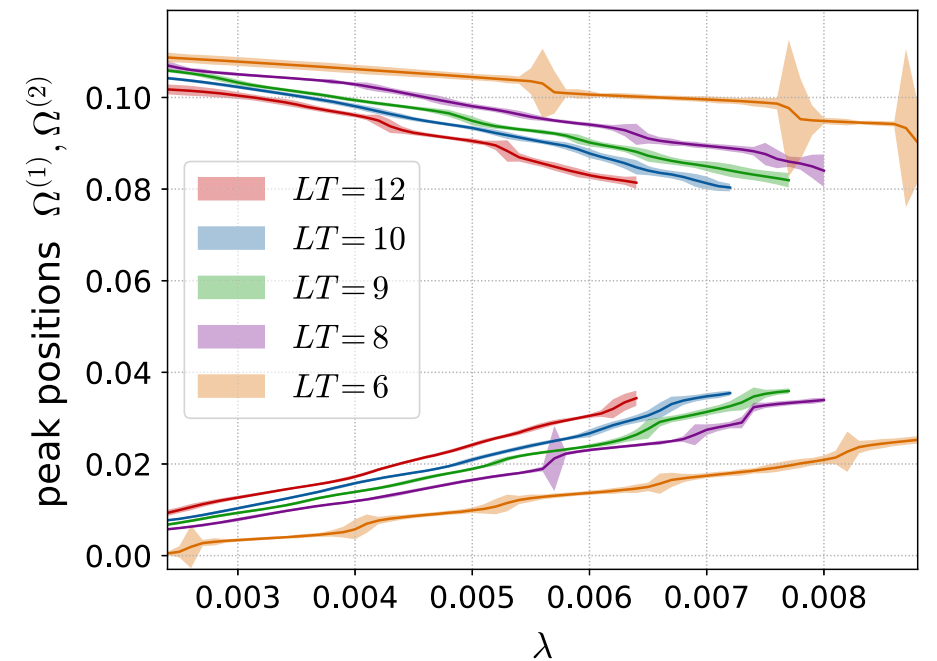
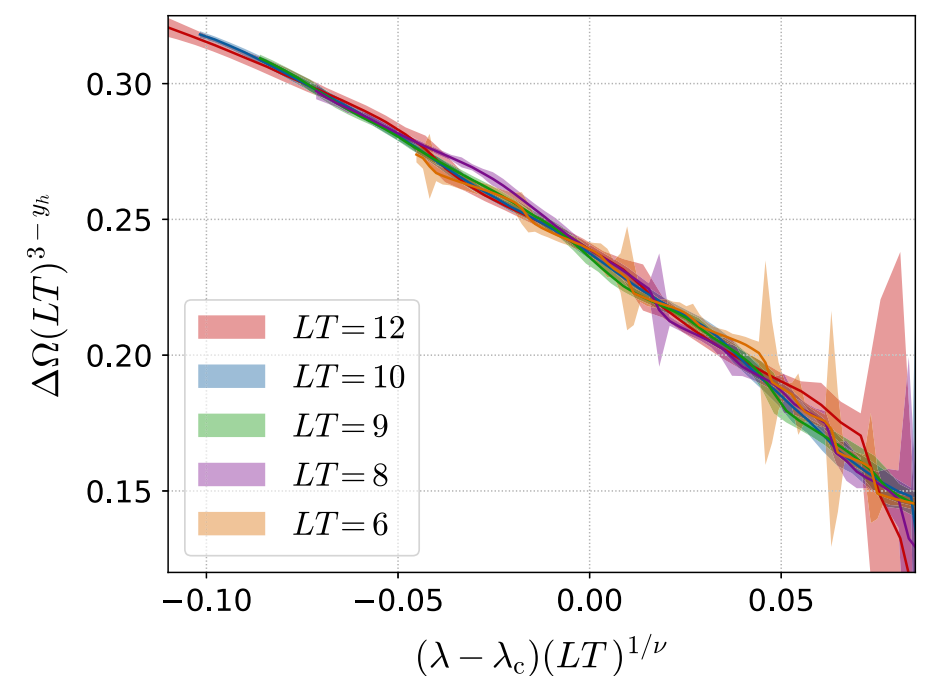


FIG. 13. Positions of peaks of the distribution function  $p(\Omega_R)$  measured on the transition line.



# backup slides

Wakabayashi, Ejiri, KK, Kitazawa (WHOT-QCD), PTEP (2022)

$W^0(4)$	288	$W^0(20)$	$1.54422361 \times 10^{14}$	$W^0(36)$	$-5.58410362 \times 10^{27}$
$W^0(6)$	8448	$W^0(22)$	$2.83682900 \times 10^{15}$	$W^0(38)$	$-2.91018925 \times 10^{29}$
$W^0(8)$	245952	$W^0(24)$	$-2.40028584 \times 10^{16}$	$W^0(40)$	$-1.50223497 \times 10^{31}$
$W^0(10)$	7372800	$W^0(26)$	$-6.88836562 \times 10^{18}$	$W^0(42)$	$-7.71380102 \times 10^{32}$
$W^0(12)$	225232896	$W^0(28)$	$-5.41133954 \times 10^{20}$	$W^0(44)$	$-3.95168998 \times 10^{34}$
$W^0(14)$	6906175488	$W^0(30)$	$-3.39122203 \times 10^{22}$	$W^0(46)$	$-2.02386871 \times 10^{36}$
$W^0(16)$	208431502848	$W^0(32)$	$-1.93668514 \times 10^{24}$	$W^0(48)$	$-1.03783044 \times 10^{38}$
$W^0(18)$	$6.00259179 \times 10^{12}$	$W^0(34)$	$-1.05424635 \times 10^{26}$	$W^0(50)$	$-5.33468075 \times 10^{39}$

$L_1^0(4, 4)$	48	$L_1^0(10, 10)$	1228.8	$L_1^0(18, 18)$	174762.67
$L_1^0(4, 6)$	1728	$L_1^0(10, 12)$	331776	$L_1^0(18, 20)$	160432128
$L_1^0(4, 8)$	45792	$L_1^0(10, 14)$	52862976	$L_1^0(18, 22)$	75497472000
$L_1^0(4, 10)$	645120	$L_1^0(10, 16)$	6258180096	$L_1^0(18, 24)$	$2.36626 \times 10^{13}$
$L_1^0(4, 12)$	-26224128	$L_1^0(10, 18)$	$5.99330 \times 10^{11}$	$L_1^0(18, 26)$	$5.50232 \times 10^{15}$
$L_1^0(4, 14)$	-3201067008	$L_1^0(10, 20)$	$4.87727 \times 10^{13}$	$L_1^0(18, 28)$	$1.01809 \times 10^{18}$
$L_1^0(4, 16)$	$-2.14087 \times 10^{11}$	$L_1^0(10, 22)$	$3.47446 \times 10^{15}$	$L_1^0(18, 30)$	$1.57315 \times 10^{20}$
$L_1^0(4, 18)$	$-1.19007 \times 10^{13}$	$L_1^0(10, 24)$	$2.20156 \times 10^{17}$	$L_1^0(20, 20)$	629145.6
$L_1^0(4, 20)$	$-6.00757 \times 10^{14}$	$L_1^0(10, 26)$	$1.24531 \times 10^{19}$	$L_1^0(20, 22)$	717225984
$L_1^0(4, 22)$	$-2.84486 \times 10^{16}$	$L_1^0(10, 28)$	$6.20798 \times 10^{20}$	$L_1^0(20, 24)$	$4.11140 \times 10^{11}$
$L_1^0(4, 24)$	$-1.28105 \times 10^{18}$	$L_1^0(10, 30)$	$2.59861 \times 10^{22}$	$L_1^0(20, 26)$	$1.54445 \times 10^{14}$
$L_1^0(4, 26)$	$-5.50874 \times 10^{19}$	$L_1^0(12, 12)$	4096	$L_1^0(20, 28)$	$4.24543 \times 10^{16}$
$L_1^0(4, 28)$	$-2.25576 \times 10^{21}$	$L_1^0(12, 14)$	1622016	$L_1^0(20, 30)$	$9.17892 \times 10^{18}$
$L_1^0(4, 30)$	$-8.69402 \times 10^{22}$	$L_1^0(12, 16)$	360603648	$L_1^0(22, 22)$	2287802.18
$L_1^0(6, 6)$	128	$L_1^0(12, 18)$	57416810496	$L_1^0(22, 24)$	3170893824
$L_1^0(6, 8)$	11520	$L_1^0(12, 20)$	$7.19497 \times 10^{12}$	$L_1^0(22, 26)$	$2.17478 \times 10^{12}$
$L_1^0(6, 10)$	716544	$L_1^0(12, 22)$	$7.51820 \times 10^{14}$	$L_1^0(22, 28)$	$9.64167 \times 10^{14}$
$L_1^0(6, 12)$	35891712	$L_1^0(12, 24)$	$6.80443 \times 10^{16}$	$L_1^0(22, 30)$	$3.09123 \times 10^{17}$
$L_1^0(6, 14)$	1464910848	$L_1^0(12, 26)$	$5.46987 \times 10^{18}$	$L_1^0(24, 24)$	8388608
$L_1^0(6, 16)$	43817011200	$L_1^0(12, 28)$	$3.96931 \times 10^{20}$	$L_1^0(24, 26)$	13891534848
$L_1^0(6, 18)$	$3.17933 \times 10^{11}$	$L_1^0(12, 30)$	$2.62442 \times 10^{22}$	$L_1^0(24, 28)$	$1.12307 \times 10^{13}$
$L_1^0(6, 20)$	$8.54676 \times 10^{13}$	$L_1^0(14, 14)$	14042.42	$L_1^0(24, 30)$	$5.80075 \times 10^{15}$



# backup slides

Wakabayashi, Ejiri, KK, Kitazawa (WHOT-QCD), *PTEP* (2022)

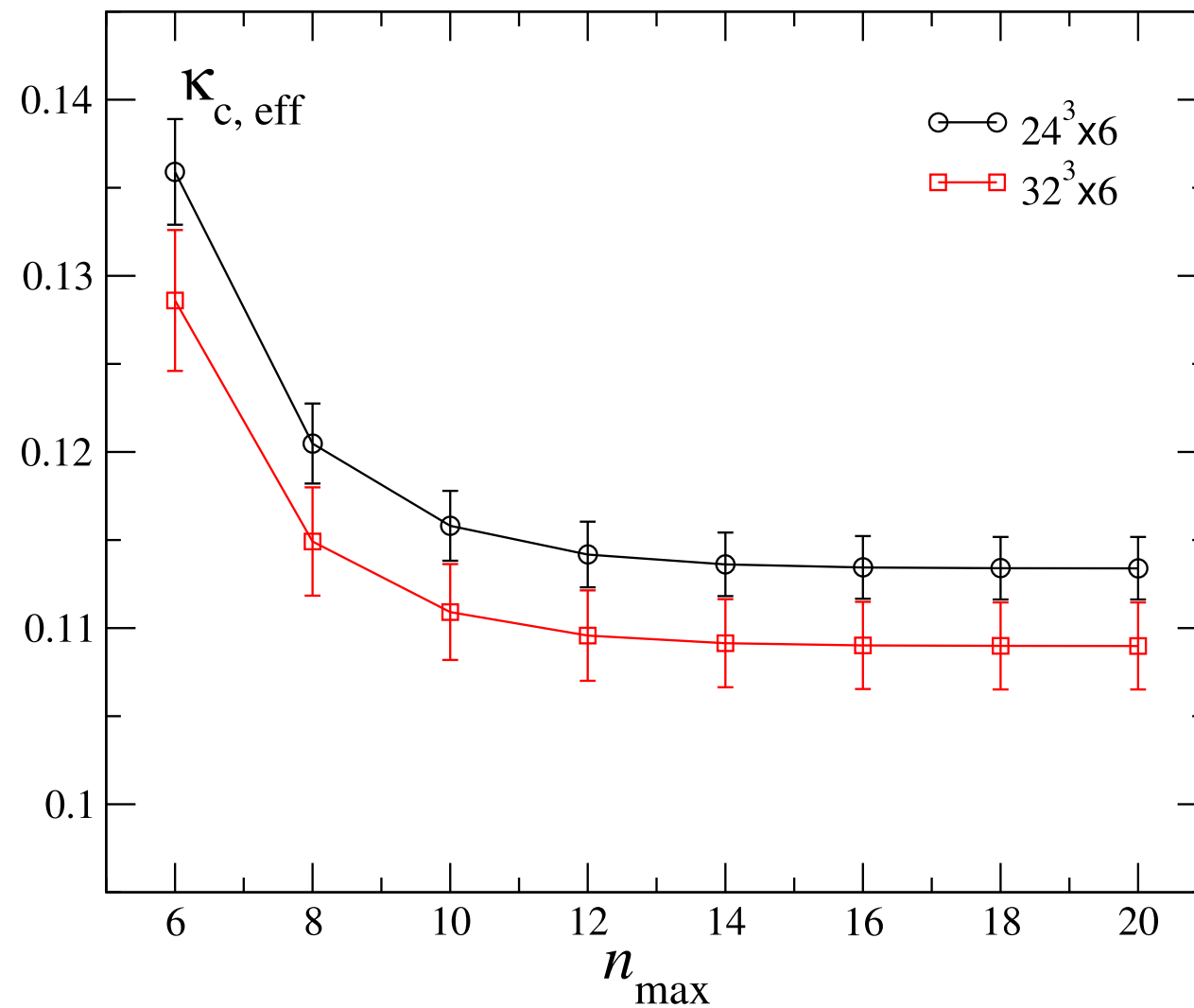


**Fig. 11.** Effective critical point  $\kappa_{c, \text{eff}}$  in two-flavor QCD for  $N_t = 6$  as a function of  $n_{\max}$ . The black circle and red square symbols are for  $\kappa_{c, \text{LO}}$  obtained on a  $24^3 \times 6$  and a  $32^3 \times 6$  lattice, respectively.

# backup slides

Wakabayashi, Ejiri, KK, Kitazawa (WHOT-QCD), *PTEP* (2022)

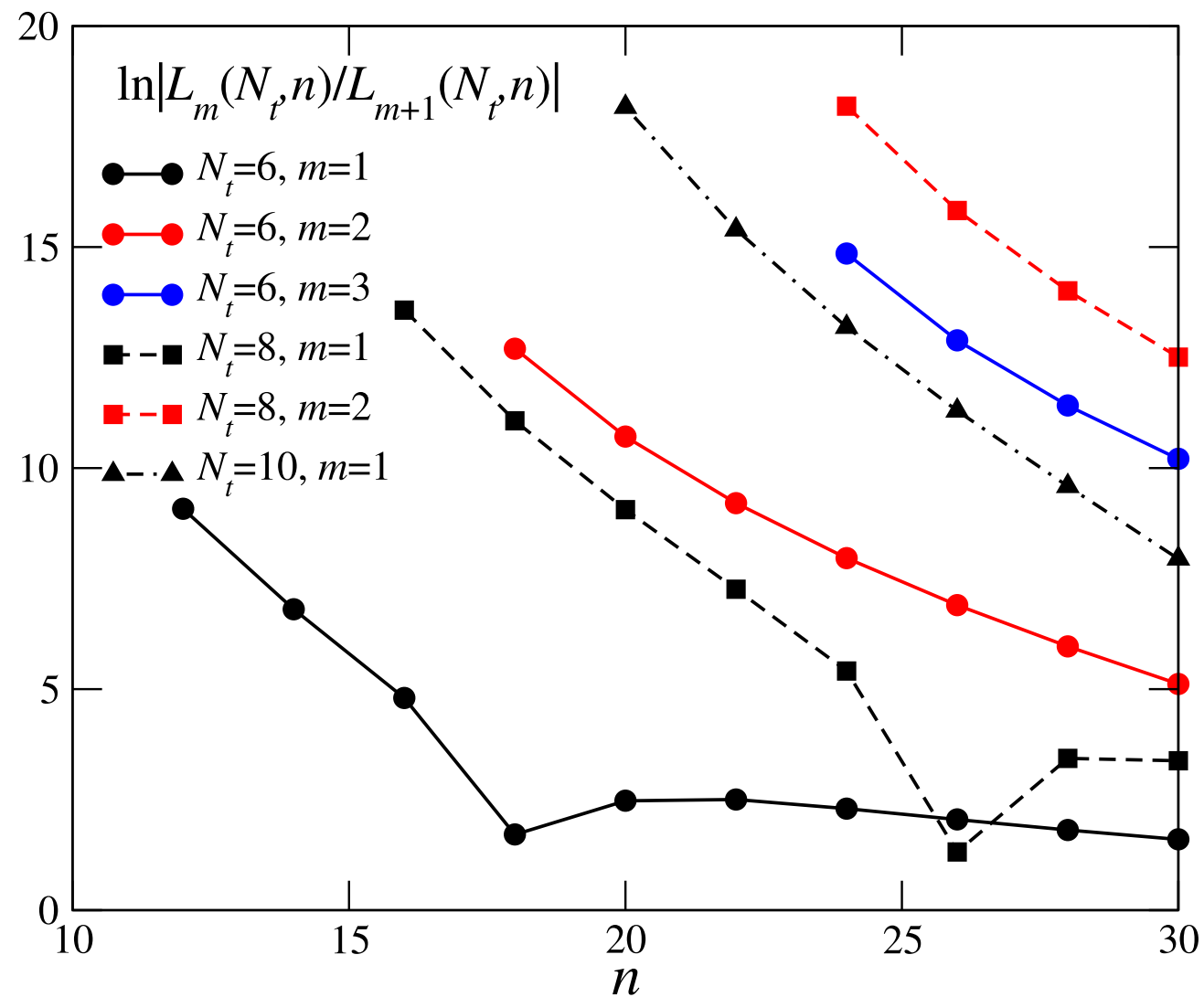


**Fig. 14.** Upper bound of  $\mu/T$  such that higher- $m$  terms are small, as given in Eq. (71).

$$\frac{\mu}{T} < \ln \left| \frac{L_m^0(N_t, n)}{L_{m+1}^0(N_t, n)} \right|$$